BAW-2245, Rev. 1
October 1995

INITIAL RT_{NDT} OF LINDE 80 WELDS BASED ON FRACTURE TOUGHNESS IN THE TRANSITION RANGE

K. K. Yoon

Prepared for
B&W Owners Group Reactor Vessel Working Group
Entergy Operations, Inc.
Commonwealth Edison Company
Duke Power Company
Florida Power Corporation
Florida Power & Light Company
GPU Nuclear Corporation
Rochester Gas & Electric Corporation
Toledo Edison Company
Virginia Power
Wisconsin Electric Power Company

B&W Document No. 43-2245-01
(See Section 8 for document signatures)

B&W NUCLEAR TECHNOLOGIES
Engineering and Project Services Division
P. O. Box 10935
Lynchburg, VA 24506-0935

EXECUTIVE SUMMARY

This document is a topical report prepared by the B&W Owners Group Reactor Vessel Working Group to justify an upper bound value for the initial reference temperature (IRT_{NDT}) for all Linde 80 weld metals and is based on fracture toughness data of these weld metals. This document is submitted to the U. S. NRC for review and acceptance as a B&W Owners Group topical report for application to the PTS rule (10CFR50.61) and 10CFR50, Appendix G, P/T limits.

The fracture toughness curves used to obtain pressure-temperature limits and for PTS evaluation are dependent on the reference temperature for nil-ductility transition (RT_{NDT}). The original method for determining initial RT_{NDT} was incorporated into Section III of the ASME Boiler and Pressure Vessel Code over 20 years ago. At that time, there was insufficient data to judge whether the Section III method for determining RT_{NDT} was appropriate for the low upper-shelf toughness weld metals used in reactor vessel fabrication. The Code method relied on the transition temperature and was based on Charpy energy values, resulting in wide scatter of initial RT_{NDT} leading to regulatory issues for the low upper-shelf Linde 80 weld metals. An alternative method for determining RT_{NDT}, based solely on the Code drop-weight test is therefore proposed. Using a new test method for fracture toughness testing in the transition range, a fracture toughness curve was generated directly from compact specimen test data. This curve was used to validate the drop-weight test data for determining an upper-bound initial RT_{NDT} value for Linde 80 weld material WF-70. This was submitted to and approved by the NRC in a topical report, BAW-2202, in 1994 (Federal Register, Vol. 59, No. 40, March 1, 1994, pages 9782~9785).

In this report, application of the alternative method for determining initial RT_{NDT}, based on additional fracture toughness tests and analyses, is expanded to cover all Linde 80 weld metals. Static fracture toughness testing was performed on several Linde 80 weld metals of representative chemical composition. Results indicate that the upper-bound RT_{NDT} is lower than the -27 F which was justified in BAW-2202 for the WF-70 Linde 80 weld metal.

It is concluded that use of an upper-bound value of -27 F with a standard deviation of zero as applied in the margin term of the NRC regulatory guide and rules is justified for all Linde 80 weld metals.

CONTENTS

1. INTRODUCTION

This document is a topical report prepared by the B&W Owners Group Reactor Vessel Working Group to justify an upper-bound value for the initial reference temperature (IRT_{NDT}) for all Linde 80 weld metals and is based on fracture toughness data of these weld metals. This revision corrects a number of typographical errors and does not contain any technical change.

In Commonwealth Edison Company's 1993 PTS submittal for Zion Unit 1, it was found that initial reference temperature for nil-ductility transition (IRT_{NDT}) value had a very wide scatter band when the Charpy transition temperature based method was applied. Using the alternative ASTM master curve approach proposed herein, the B&W Owners Group Reactor Vessel Working Group (RVWG) has demonstrated that the IRT_{NDT} values obtained from drop-weight test data are more reliable and justify that the IRT_{NDT} of WF-70 weld is -27 F. This was documented in a topical report (BAW-2202[1]) and submitted to the NRC staff for their review; the topical report was accepted in 1994 (Federal Register, Vol. 59, No. 40, March 1, 1994, pages 9782~9785). Accordingly, the NRC granted an exemption to Commonwealth Edison Company allowing use of the IRT_{NDT} value of -27 F for WF-70 weld metal.

This regulatory action resulted in another Linde 80 weld material becoming the limiting weld in the Zion Unit 1 reactor vessel. This prompted the RVWG to investigate other Linde 80 welds to determine whether this alternative approach can be applied to all Linde 80 welds. The IRT_{NDT} values of these welds are currently controlled by Charpy 50 ft-lb transition temperature.

The RVWG inventoried all archive Linde 80 weld materials and generated a test matrix based on material availability. Fracture toughness tests were performed to obtain fracture toughness values in the transition range. The results were analyzed using the same master curve method that was used for the Zion Unit 1 WF-70 weld; the resulting master curves are compared with that of WF-70. It was demonstrated that all Linde 80 weld metals can conservatively be represented by WF-70 fracture toughness in the transition range.

2. LINDE 80 WELD MATERIAL

This Section provides the necessary assurance that the materials studied in this effort are representative of Linde 80 welds generally.

The reactor vessel shells of interest that were fabricated by Babcock & Wilcox were automatic submerged-arc welded with Mn-Mo-Ni low alloy steel consumable wire and Linde 80 flux. The weld wire was copper coated, introducing variable amounts of copper into the melt. Linde 80 flux is a neutral flux, that is, it does not influence the metallic element composition of the weld. Each particular combination of wire heat and flux lot was uniquely identified with either an "SA" or "WF" number and subjected to weld qualification testing. The reactor vessel beltline welds are identified in Table 2-1[2] and their chemical compositions are shown in Table 2-2[2]. The mean, median, range, and standard deviation of the individual elements do not show great variation, except perhaps for copper content. Considering that the vessels were similarly fabricated, the welds may reasonably be regarded to be a "family" that in the unirradiated condition should have similar mechanical and fracture toughness properties.

The chemical composition of the test specimen materials are shown in Table 2-3[3]. The test specimen materials are reasonably representative of the beltline material when considering the mean and range values for the individual elements.

One test of the "family" supposition expressed above is the closeness of tension test results for the various wire/flux combinations. Table 2-4[4] shows room temperature tensile values for 14 wire/flux combinations and Table 2-5[4] shows elevated temperature values for 12 wire/flux combinations. (These values are for surveillance material, and since the same material was used for more than one plant, there is more than one entry for some wire/flux combinations.) These test values were obtained over a long period of time, with testing at more than one laboratory using hydraulic and electric testing machines. Elevated temperature testing was performed at 570 F to 600 F. Inspection of the values shows them to be sufficiently close,

especially when considering the possible variability in testing, to support the premise that Linde 80 welds are a "family" of materials.

Table 2-1 Beltline Linde 80 Weld Identification

Weld Material	Wire Heat	Flux Lot	Reactor
SA-775	1P061	8304	PB-1
SA-812	1P0815	8350	PB-1
SA-847	61782	8350	Ginna, PB-1
SA-1073	1P0962	8445	Oc-1
SA-1101	71249	8445	Ginna, PB-1, TP-3, TP-4
SA-1135	61782	8457	Oc-1
SA-1229	71249	8492	Oc-1
SA-1426	8T1762	8553	Oc-1, PB-1
SA-1430	8T1762	8553	Oc-1
SA-1484	72442	8579	PB-2, TP-3
SA-1493	8T1762	8578	Oc-1
SA-1494	8T1554	8579	Surry-1, TMI-1
SA-1526	299L44	8596	Surry-1, TMI-1
SA-1580	8T1762	8596	CR-3
SA-1585	72445	8597	Oc-1, Surry-1, -2
SA-1650	72445	8632	Surry-1
SA-1769	71249	8738	CR-3, Zion-1, -2
WF-4	8T1762	8597	Surry-2, Zion-1
WF-8	8T1762	8632	CR-3, Surry-2, TMI-1, Zion-1
WF-18	8T1762	8650	ANO-1, CR-3
WF-25	299L44	8650	Oc-1, -2, TMI-1
WF-29	72102	8650	Zion-2
WF-67	72442	8669	Oc-3, TP-4
WF-70	72105	8669	CR-3, Oc-3, TMI-1, TP-4, Zion-1, -2
WF-112	406L44	8688	ANO-1
WF-154	406L44	8720	Oc-2, Zion-1
WF-169-1	8T1554	8754	CR-3
WF-182-1	821T44	8754	ANO-1, Davis-Besse
WF-200	821T44	8773	Oc-3, Zion-2
WF-232	8T3914	8790	Davis-Besse
WF-233	T29744	8790	Davis-Besse

Table 2-2 Linde 80 Beltline Weld Metal Composition (Weight Percent)

Weld Material	C	Mn	P	S	Si	Cr	Ni	Mo	Cu
SA-775	0.08	1.52	0.024	0.019	0.46	0.06	0.63	0.45	0.19
SA-812	0.08	1.54	0.017	0.015	0.40	0.07	0.52	0.38	0.17
SA-847	0.08	1.34	0.012	0.012	0.45	0.08	0.54	0.38	0.25
SA-1073	0.10	1.38	0.025	0.017	0.51	0.11	0.64	0.43	0.21
SA-1101	0.07	1.28	0.021	0.014	0.52	0.16	0.60	0.37	0.26
SA-1135	0.08	1.45	0.011	0.013	0.49	0.08	0.64	0.38	0.25
SA-1229	0.06	1.56	0.021	0.012	0.43	0.16	0.61	0.37	0.26
SA-1426	0.08	1.53	0.017	0.013	0.43	0.12	0.55	0.41	0.20
SA-1430	0.08	1.43	0.017	0.015	0.43	0.12	0.55	0.41	0.20
SA-1484	0.08	1.52	0.018	0.015	0.42	0.09	0.60	0.39	0.24
SA-1493	0.08	1.51	0.017	0.010	0.46	0.12	0.55	0.41	0.20
SA-1494	0.09	1.52	0.015	0.012	0.44	0.08	0.63	0.37	0.18
SA-1526	0.09	1.53	0.013	0.017	0.53	0.09	0.68	0.42	0.35
SA-1580	0.07	1.45	0.015	0.013	0.43	0.12	0.55	0.41	0.20
SA-1585	0.08	1.45	0.016	0.016	0.51	0.09	0.59	0.38	0.21
SA-1650	0.09	1.43	0.018	0.014	0.40	0.09	0.59	0.38	0.21
SA-1769	0.09	1.49	0.020	0.014	0.56	0.16	0.61	0.37	0.26
WF-4	0.07	1.48	0.017	0.011	0.51	0.12	0.55	0.41	0.20
WF-8	0.06	1.45	0.009	0.009	0.53	0.12	0.55	0.41	0.20
WF-18	0.09	1.45	0.004	0.017	0.39	0.12	0.55	0.41	0.20
WF-25	0.09	1.60	0.015	0.016	0.50	0.09	0.68	0.42	0.35
WF-29	0.08	1.65	0.015	0.012	0.42	0.05	0.63	0.38	0.23
WF-67	0.08	1.55	0.021	0.016	0.58	0.09	0.60	0.39	0.24
WF-70	0.09	1.63	0.018	0.009	0.54	0.10	0.59	0.40	0.35
WF-112	0.08	1.47	0.016	0.015	0.54	0.07	0.59	0.40	0.31
WF-154	0.07	1.54	0.013	0.016	0.42	0.07	0.59	0.40	0.31
WF-169-1	0.08	1.56	0.016	0.016	0.45	0.08	0.63	0.37	0.18
WF-182-1	0.08	1.69	0.014	0.013	0.45	0.14	0.63	0.40	0.24
WF-200	0.07	1.60	0.010	0.015	0.48	0.14	0.63	0.40	0.24
WF-232	0.06	1.30	0.016	0.011	0.47	0.11	0.64	0.37	0.18
WF-233	0.05	1.45	0.021	0.015	0.42	0.08	0.68	0.44	0.29
Mean	0.08	1.50	0.02	0.01	0.47	0.10	0.60	0.40	0.24
Std. Dev.	0.011	0.093	0.004	0.002	0.051	0.029	0.043	0.021	0.051
Max.	0.10	1.69	0.025	0.019	0.58	0.16	0.68	0.45	0.35
Min.	0.05	1.30	0.004	0.009	0.39	0.05	0.52	0.37	0.17

Table 2-3 Chemical Composition of Test Specimen Material (Weight Percent)

Weld Material	C	Mn	P	S	Si	Cr	Ni	Mo	Cu
SA-1526	0.09	1.53	0.013	0.017	0.53	0.09	0.68	0.42	0.35
WF-25	0.09	1.60	0.015	0.016	0.50	0.09	0.68	0.42	0.35
WF-70	0.09	1.63	0.018	0.009	0.54	0.10	0.59	0.40	0.35
WF-112	0.08	1.47	0.016	0.015	0.54	0.07	0.59	0.40	0.31
WF-193	0.09	1.49	0.016	0.016	0.51	0.06	0.59	0.39	0.28
Mean	0.09	1.57	0.02	0.01	0.51	0.09	0.63	0.41	0.3
Std. Dev.	0.005	0.078	0.002	0.003	0.031	0.025	0.040	0.011	0.042

Table 2-4 Tension Test Data at Room Temperature

Weld Material	Ultimate Tensile Strength (ksi)	Yield Strength (ksi)	Uniform Elongation (%)	Total Elongation (%)	Reduction in Area (%)
SA-1036	87.4	73.5		22.8	62.0
SA-1094	90.8	70.2		23.8	64.8
SA-1101	92.8	76.3		24.9	64.1
SA-1135	84.6	67.0	9.3	17.7	66.7
SA-1263	86.3	69.9		25.5	65.1
SA-1526	83.2	69.7	15.2	26.5	66.7
SA-1585	78.2	61.3	10.0	23.0	67.0
WF-25	80.2	64.9	9.0	26.0	67.0
WF-25	86.2	69.2	12.6	26.7	62.8
WF-67	86.2	71.0	8.0	20.0	66.0
WF-70	92.7	77.4	8.0	16.0	63.0
WF-112	80.5	63.3	16.9	30.9	63.7
WF-182-1	85.6	70.2	15.1	26.6	64.2
WF-193	87.0	71.9	16.2	27.1	64.1
WF-193	83.4	67.5	16.2	29.0	63.0
WF-193	84.6	67.6	12.3	28.1	64.0
WF-209-1	89.4	72.7	15.0	25.8	62.7
WF-209-1	88.8	73.6	14.6	25.6	63.6
WF-209-1	95.2	81.4	10.7	25.6	57.9
WF-209-1	90.5	75.0	12.5	28.1	62.9
Mean	86.7	70.7	12.6	25.0	64.1
Std. Dev.	4.3	4.7	3.0	3.6	2.1

Table 2-5 Elevated Temperature Tension Test Data

Weld Material	Test Temp. (F)	Ultimate Tensile Strength (ksi)	Yield Strength (ksi)	Uniform Elongation (%)	Total Elongation (%)	Reduction in Area (%)
SA-1036	600	80.4	59.2		20.7	56.1
SA-1094	600	82.2	60.7		20.8	55.1
SA-1101	600	88.0	67.6		21.3	58.7
SA-1263	600	83.6	62.6		20.3	58.1
SA-1526	600	79.0	58.1	14.2	22.9	62.0
SA-1585	580	76.1	57.9	9.0	20.0	59.0
WF-25	580	75.3	60.3	6.0	16.0	59.0
WF-25	570	81.7	64.3	9.5	20.5	52.3
WF-25	600	82.0	60.8			54.0
WF-67	580	76.9	57.0	7.0	17.0	59.0
WF-112	600	80.8	56.4	16.8	24.4	61.0
WF-182-1	580	83.2	67.6	12.9	18.8	50.2
WF-193	600	84.9	63.1	14.7	22.9	54.6
WF-193	580	80.6	61.6	13.7	20.5	52.3
WF-193	570	81.4	60.4	10.8	21.9	52.1
WF-209-1	600	87.7	66.5	13.2	21.0	50.3
WF-209-1	600	85.0	65.1	12.8	21.0	55.6
WF-209-1	580	89.7	69.8	10.4	20.6	48.9
WF-209-1	580	87.9	67.4	10.9	21.4	52.1
Mean		82.4	62.4	11.6	20.7	55.3
Std. Dev.		4.0	3.9	2.9	1.9	3.8

3. DETERMINATION OF RT_{NDT}

3.1 General

RT_{NDT} is an integral part of the ASME B&PV Code reference fracture toughness curves in Appendix G to Section III and Appendices A and G to Section XI of the ASME Code. RT_{NDT} is used as an index to predict degradation of fracture toughness caused by irradiation embrittlement. As fluence increases, the RT_{NDT} increases, and the toughness curve shifts to the right as shown in Figure 3-1. This yields a reduction in toughness at a given temperature as the neutron fluence in the material is increased. RT_{NDT} is an essential input for determining plant operation pressure-temperature limits and RT_{PTS} (the PTS screening criteria under 10 CFR 50.61[5]). Rules to determine RT_{NDT} are provided by Regulatory Guide 1.99, Revision 2[6]. In the regulatory guide, the adjusted RT_{NDT} is defined as follows:

$$RT_{NDT} = IRT_{NDT} + \Delta RT_{NDT} + \text{Margin}$$

where IRT_{NDT} is the initial RT_{NDT}, and ΔRT_{NDT} is the shift in RT_{NDT} due to irradiation and is a function of fluence and chemical composition of the material. Margin is defined as follows:

$$\text{Margin} = 2\sqrt{\sigma_I^2 + \sigma_\Delta^2}$$

where σ_I and σ_Δ are the standard deviations of IRT_{NDT} and shift data populations.

IRT_{NDT} is determined in accordance with NB-2331 of Section III of the ASME B&PV Code and is the focus of this report because of the difficulty in its application to the Linde 80 weld metal family.

3.2 Current Methodology - NB-2331

The RT_{NDT} value for unirradiated material is defined as initial RT_{NDT} (IRT_{NDT}) in Regulatory Guide 1.99, Revision 2. The procedure to obtain IRT_{NDT} is specified in NB-2331 of Section III of the ASME B&PV Code. Two types of tests are required: Charpy V-notch impact tests and drop-weight tests. A Charpy impact energy curve is drawn as a function of temperature and a transition temperature is determined from this curve at the 50 ft-lb impact energy level. From the drop-weight tests, the nil-ductility temperature (T_{NDT}) is obtained. The T_{NDT} is compared with the 50 ft-lb Charpy transition temperature minus 60 F. The greater of these two values is selected as the RT_{NDT} of the material.

When the reference fracture toughness curve of WRC-175[7] was prepared under the HSST Program, all the ferritic vessel steel data were T_{NDT} controlled. The first plot of fracture toughness data as shown in Figure 3-2 has the abscissa labeled as $T-T_{NDT}$ indicating that for these materials the Charpy transition temperature at 50 ft-lb did not control the initial RT_{NDT} values. There was little information available then regarding irradiated specimen fracture toughness data of low upper-shelf toughness materials like Linde 80 weld metal, especially how accurately the Charpy 50 ft-lb transition temperature would index irradiation induced embrittlement.

3.3. B&W Owners Group WF-70 Weld

In response to the NRC's concern over the initial RT_{NDT} values for Linde 80 weld metal WF-70, the B&W Owners Group conducted a number of tests and analyses of WF-70 weld metal. IRT_{NDT} values of WF-70 weld metal were all based on the Charpy transition temperature. From these data, it is seen that the IRT_{NDT} values have a large scatter (standard deviation of 35 F). This scatter is much larger than that observed in the irradiated Charpy data. This leads to questioning the applicability of the current NB-2331 method for determining IRT_{NDT} of low upper-shelf toughness materials.

In 1992, ORNL conducted a large test program to determine RT_{NDT} values for WF-70 weld metal obtained from the Midland Unit 1 vessel beltline and nozzle belt. The results are reported in NUREG/CR-5914[8]. Charpy impact energy test data were collected for a number of cross-sections. The resulting IRT_{NDT} values, based on Charpy transition temperatures, are plotted in Figure 3-3 as a function of the location through the radial direction in the Midland reactor vessel wall. As can be seen from this figure, the IRT_{NDT}

values fluctuate greatly through the wall. For IRT_{NDT} to be a useful material parameter, its value should be independent of the location from where the specimens are obtained. This extreme variability of RT_{NDT} from the same cross-section indicates the inadequacy of the NB-2331 method. To develop an alternative approach, exclusive use of the drop-weight test data (without the Charpy 50 ft-lb transition temperature) was explored to index the Code fracture toughness curve with a fracture toughness curve generated by the master curve method[1] using directly measured fracture toughness data. Additional drop-weight test data were obtained from the ORNL test program[8] and found to be similar to the RVWG drop-weight test data.

The test results yielded a mean T_{NDT} value of the combined data set of -56.0 F with a standard deviation of 14.8 F. The IRT_{NDT} was determined according to Regulatory Guide 1.99, Revision 2 as follows:

$$RT_{NDT} = IRT_{NDT} + \Delta RT_{NDT} + \text{Margin}$$

For an unirradiated weld metal

$$\Delta RT_{NDT} = 0$$

$$\sigma_\Delta = 0$$

$$\text{Margin} = 2\sqrt{\sigma_I^2 + \sigma_\Delta^2} = 2\sigma_I$$

and therefore, $RT_{NDT} = -56.0 + 2(14.8) = -26.4$ F ~-27 F.

To demonstrate adequacy of the alternative method for determining IRT_{NDT}, the K_{IR} curve using the above RT_{NDT} value of -27 F is plotted with the master curve generated from the WF-70 static fracture toughness data in Figure 3-4. It is clear that this K_{IR} curve lower bounds the 5% confidence limit curve. Therefore, the proposed RT_{NDT} approach was concluded to be valid for the WF-70 transition range fracture toughness. ORNL and the Westinghouse Owners Group (WOG) also conducted fracture toughness tests in the transition range for WF-70 weld material obtained from the Midland Unit One reactor vessel. The WOG data[9] was compared with the RVWG master curve for WF-70 in Figure 3-5 with very good agreement.

Figure 3-1 Fracture Toughness Curve Shift due to Irradiation Embrittlement

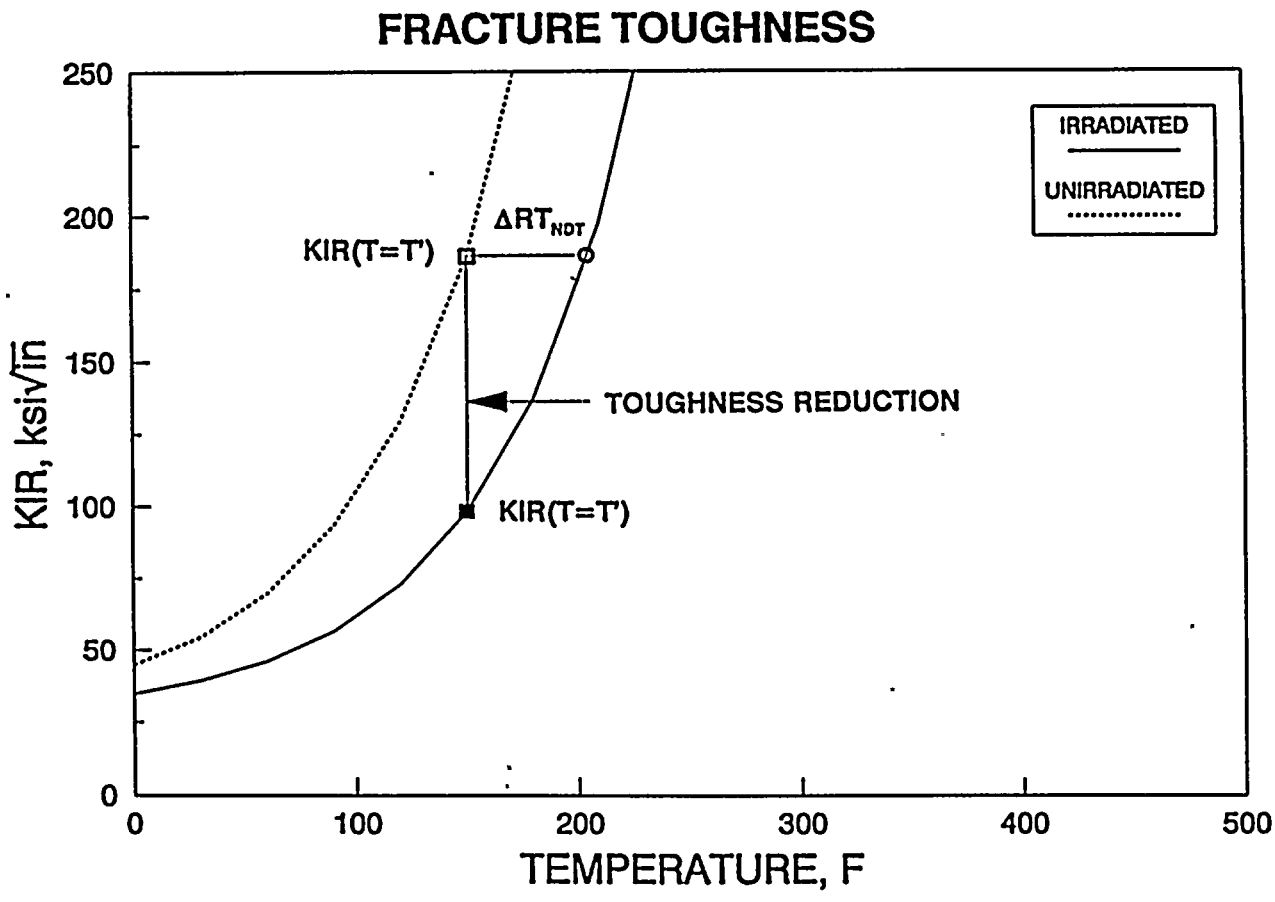

Figure 3-2 Derivation of Fracture Toughness Reference Curve K_{IR}

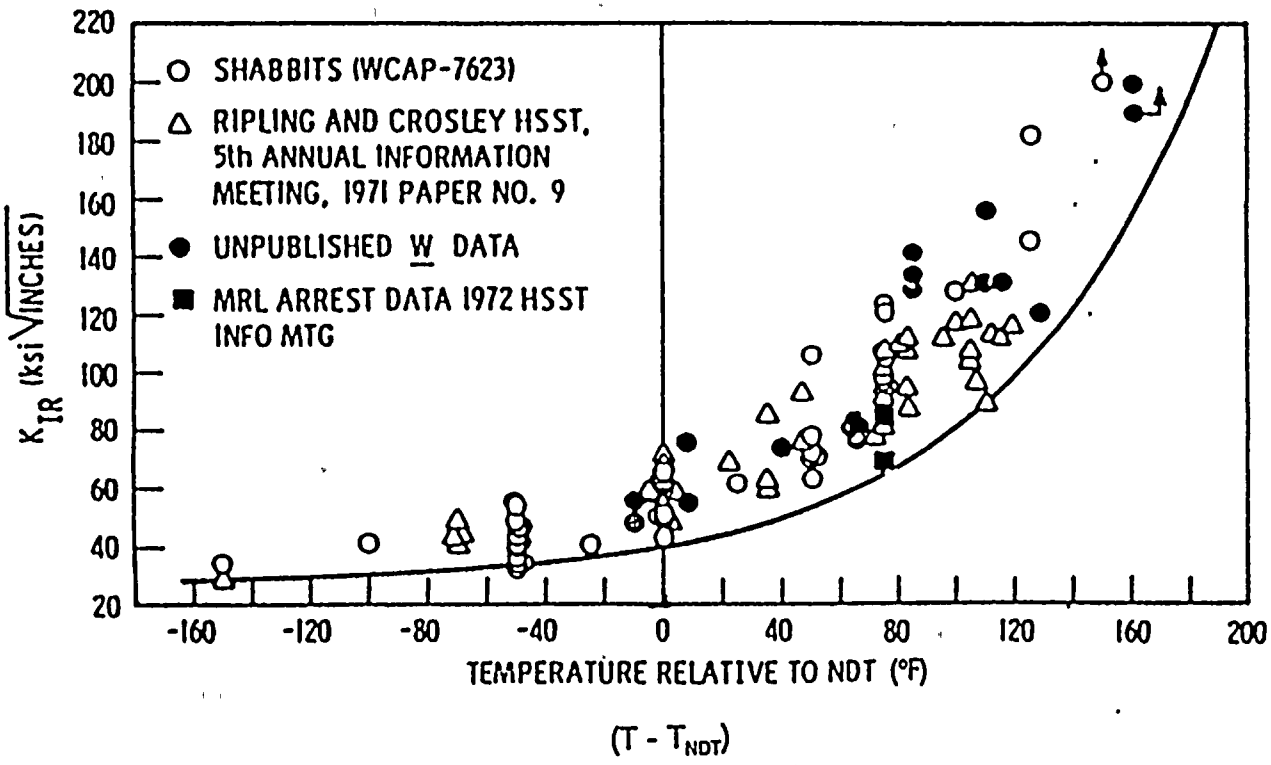

Figure 3-3 RT_{NDT} at Midland Weld Cross-Sections

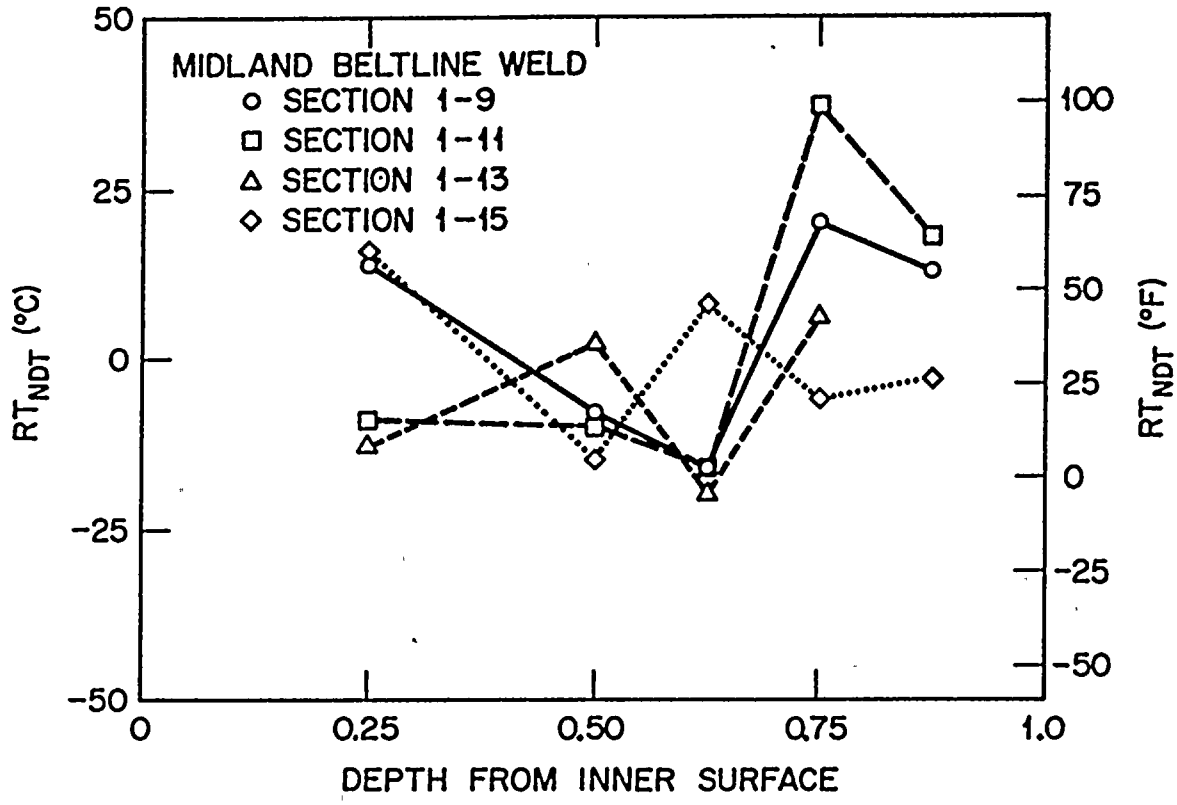

Figure 3-4 WF-70 Master Curve and Code Reference Toughness Curves

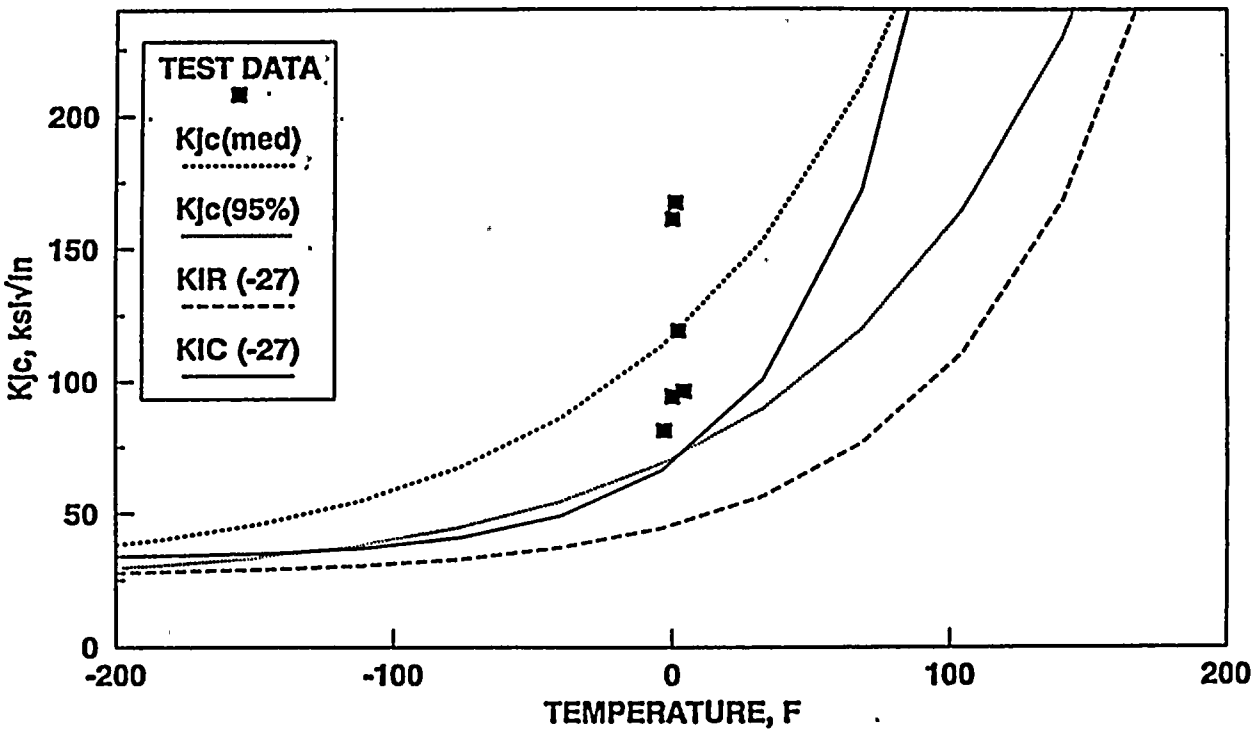

Figure 3-5 WF-70 Fracture Toughness Comparison

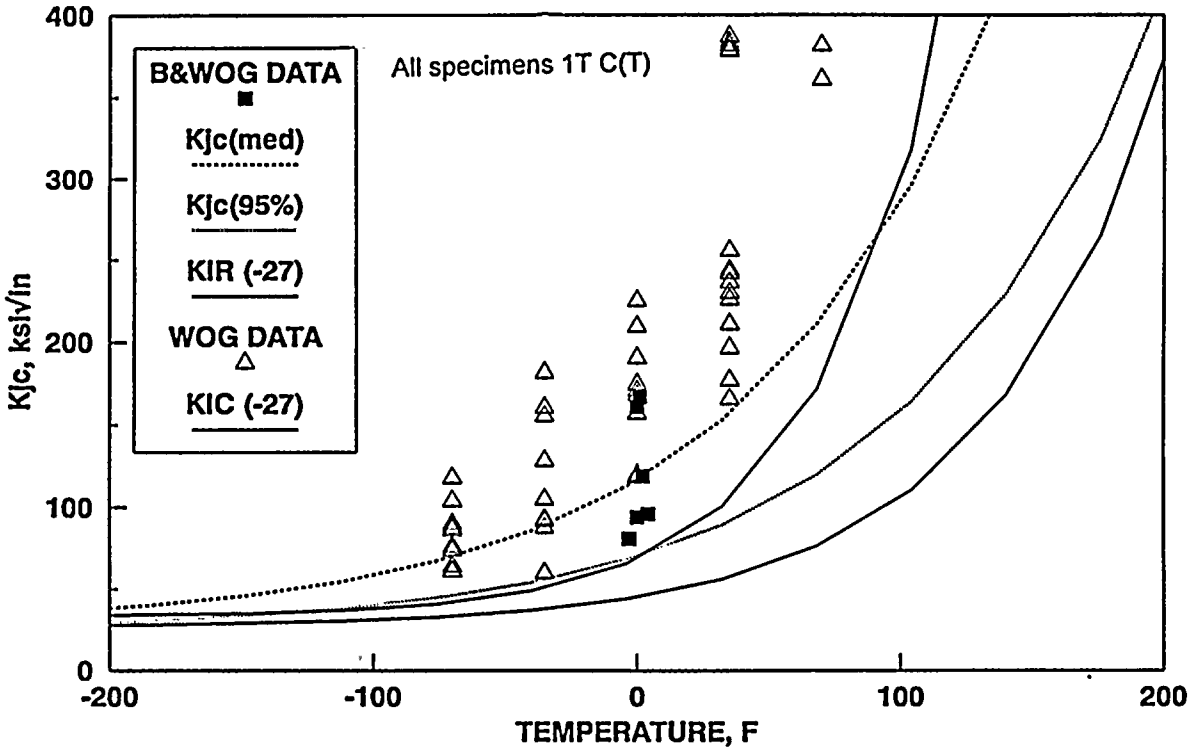

4. FRACTURE TESTING OF LINDE 80 WELDS

For the Zion Unit 1 reactor vessel, adoption of the alternatively determined IRT_{NDT} value removed the WF-70 weld from being the limiting material and another Linde 80 weld became the new limiting material for all P-T limit and PTS issues for the reactor vessel. This prompted the RVWG to investigate the remaining Linde 80 welds to determine whether the alternative approach can also be applied to them. The IRT_{NDT} values of all of these welds are currently controlled by Charpy transition temperature.

4.1. Method for Fracture Toughness in Transition Range - Master Curve Approach

ASTM Committee E-08 on Fatigue and Fracture has been developing a standard for a test method to determine fracture toughness in the transition range using a limited number of specimens. Draft No. 10 of this proposed standard is shown in Appendix A and was used for this validation effort. This method requires the testing of a minimum of six compact or three-point bend specimens of the material of interest at a temperature where the material exhibits fracture toughness of approximately 100 MPa$\sqrt{m}$ (90.9 ksi$\sqrt{in}$). The standard compact specimen size is 1T but other specimen sizes can be used with the prescribed size correction. Side grooving is optional. The J-integral is calculated in accordance with ASTM E 813-89 and the J at cleavage fracture is defined as J_c. Plane stress fracture toughness, K_{jc}, is obtained by the following relationship:

$$K_{jc} = \sqrt{J_c E} \qquad (4\text{-}1)$$

where E is the Young's modulus. At 0 F, 30,200 ksi is a representative Young's modulus for Linde 80 weld material.

The procedure requires pop-in discontinuity and constraint checks; sufficient constraint should exist at the onset of cleavage fracture. Data censoring is required based on constraint conditions at the crack tip, however, this requirement is still an unresolved issue. According to the Weibull plots of all B&W Owners Group data, all data points are acceptable.

This procedure yields a master transition temperature curve;

$$K_{jc(med)} = 30 + 70 \exp[0.019(T - T_o)], \quad \text{Mpa}\sqrt{m} \qquad (4\text{-}2)$$

where $K_{jc(med)}$ - median fracture toughness

T - test temperature, C

T_o - reference temperature

$$T_o = T - (0.019)^{-1} \ln\{[K_{jc(med)} - 30]/70\},\ C. \quad (4\text{-}3)$$

The procedure also provides equations to obtain confidence limit curves. A 5% confidence limit is taken as a lower limit curve for comparison purpose. The code K_{IC} and K_{IR} curves are given by the following equations:

$$K_{Ic} = 2.806 \exp [0.02(T - RT_{NDT} + 100)] + 33.2,\ ksi\sqrt{in} \quad (4\text{-}4)$$

$$K_{IR} = 1.223 \exp [0.0145(T - RT_{NDT} + 160)] + 26.78,\ ksi\sqrt{in} \quad (4\text{-}5)$$

where T is temperature in F.

4.2 Material Availability and Test Matrix

The test matrix in Table 4-1 was prepared for the additional testing of Linde 80 welds, based on availability of Linde 80 weld material for specimen fabrication and on consideration of material representation.

Table 4-1. Test Matrix

Weld Metal	Chemical Composition		Static Tests
	Cu wt%	Ni wt%	1/2T C(T)
WF-112	0.32	0.59	6
SA-1526	0.37	0.7	6
WF-182-1	0.21	0.63	6
WF-193	0.28	0.54	6
WF-25	0.35	0.7	6
WF-70	0.35	0.59	2
Total	-	-	32

4.3 Test Temperature

The Westinghouse Owners Group tested a large number of 1T C(T) specimens fabricated from the Midland reactor vessel beltline WF-70 weld[9]. The tests were conducted at five different temperatures as shown in Figure 3-5. In order to demonstrate the sensitivity of the test temperature with regard to master

curves, three test temperatures were selected for application of the master curve method. The remaining two higher temperatures were not used since the mean toughness is too high for the master curve approach and would involve large amounts of ductile tearing.

Figure 4-1 shows three median Kjc curves based on data from the WOG WF-70 fracture tests at three different test temperatures, 0 F, -35 F and -70 F. These curves are very close to each other, indicating that for as long as the fracture toughness range is close to the recommended value in the master curve approach, the resulting Kjc curves will be adequate for the material tested.

In BAW-2202, both 1/2T C(T) and 1T C(T) specimens of WF-70 were used for the static testing. All six 1T C(T) specimens tested at 0 F yielded good results, however, five out of six 1/2T C(T) specimens that were tested at 0 F resulted in excessive ductile tearing which invalidated the data. The WOG data shown in Figure 3-5 has satisfactory test temperatures of 0, -35 and -70 F. All specimens were 1 inch thick. To conserve the remaining archive materials of Linde 80 welds, all specimens were fabricated to a 1/2T size. To prevent excessive tearing, the test temperature was selected to be -70 F. The proposed standard requires the testing of six specimens at one temperature; K_{jc} data is determined from J at cleavage fracture.

4.4. Static Fracture Toughness

Two of the WF-70 1/2T C(T) specimens were tested at -70 F to confirm the adequacy of the selected test temperature for the 1/2T size specimens. These two data points were compared with the WF-70 master curve in Figure 4-2 showing very good agreement. These points are very close to the median curve. The remaining specimens were then also tested at -70 F and the results are shown in Table 4-2 and plotted in Figure 4-3; this includes the WF-70 data that were reported in BAW-2202.

4.5 Data Analysis

The Weibull plot and master curve for each of the five Linde 80 weld metals are shown in Figures 4-4 through 4-13. Each Weibull plot clearly shows good data fit to a slope of 4. This indicates that the master curve method can be applied to this data set.

Since only one test temperature was selected for each of these welds, the uncertainty associated with reference temperature and the accompanying margin term discussed in the proposed ASTM standard is not applicable. However, this concept can be inversely applied to prove that these individual master curves are

for a family of similar materials. If variability of reference temperature is relatively small, then these materials can be considered as the same family of materials.

Reference temperature, T_o, is defined in equation 16 of the proposed standard,

$$T_o = T - (0.019)^{-1} \ln [(Kjc(med) - 30)/70], \ C$$

where T is the test temperature and Kjc(med) is the median value of Kjc for 1T specimens. T_o should be relatively independent of the test temperature chosen. If the T_o values from these tests are very different, it probably indicates that the data group do not fit one master curve.

In the master curve equation, equation 4-2, the reference temperature can be seen to be a shift parameter similar to RT_{NDT} in the Code reference fracture toughness equation. By design, the form of this median toughness curve resembles the Code reference fracture toughness equation.

Table 4-3 shows T_o values for the five Linde 80 welds tested. The mean value is -80 C (-112 F) with a standard deviation of 8.5 C (15.3 F). It must, therefore, be inferred that this group behaves like one material.

Recently, ORNL tested Linde 80 weld metals (63W, 64W, and 65W) in the transition range and the resulting data were analyzed[10] for their master curves. The reference temperatures calculated from these data are also included in Table 4-3 which show a mean reference temperature of -72 C (-98 F) with a standard deviation of 10.2 C (18.4 F), which also indicates that they are of the same material family in terms of fracture toughness in the transition range. The combined mean and the standard deviation are -77.1 C (-106.7 F), and 9.3 C (16.8 F) as presented in Table 4-4. On the other hand, WF-70 is an exceptional case. The toughness of this weld seems slightly lower than the other Linde 80 welds. The data reported in BAW-2202, for tests at 0 F, show a mean reference temperature of -32 C (-25.6 F). This is somewhat higher than the rest of the materials. This indicates that the WF-70 toughness curve will lower bound all other Linde 80 welds as illustrated in Section 5.

Table 4-2 Static Fracture Toughness Data

Weld Metal	Specimen Number	K_{jc}(0.5T) MPa$\sqrt{m}$	K_{jc}(0.5T) ksi$\sqrt{in}$
WF-25	1	100	91
	2	109	99
	3	117	106
	4	117	107
	5	184	167
	6	200	182
	average	138	126
SA-1526	1	100	91
	2	149	136
	3	150	136
	4	155	141
	5	164	149
	6	172	157
	average	148	135
WF-193	1	114	103
	2	155	141
	3	159	145
	4	165	150
	5	204	186
	6	229	208
	average	171	156

Table 4-2 Static Fracture Toughness Test Data (Cont'd)

Weld Metal	Specimen Number	K_{jc}(0.5T) MPa$\sqrt{m}$	K_{jc}(0.5T) ksi$\sqrt{in}$
WF-182-1	1	116	105
	2	149	135
	3	156	142
	4	161	147
	5	181	165
	6	193	175
	average	159	145
WF-112	1	128	116
	2	169	154
	3	189	172
	4	205	186
	5	208	189
	6	237	216
	average	189	172

Table 4-3 Reference Temperatures for Linde 80 Welds

1995 RVWG Test Data		
Weld Metal	T_o, C	T_o, F
WF-25	-68.8	-91.8
SA-1526	-75.5	-103.9
WF-193	-84.1	-119.4
WF-182-1	-80.3	-112.5
WF-112	-91.1	-132.0
Mean	-80.0	-111.9
Standard Deviation	8.5	15.2
1995 ORNL Test Data		
ORNL 63W, -75 °F	-73.1	-99.6
ORNL 64W, -58 °F	-61.6	-78.9
ORNL 65W, -94 °F	-82.0	-115.6
ORNL Mean	-72.2	-98.0
ORNL Standard Deviation	10.2	18.4
1993 WOG Data		
WF-70 (WOG), 0 °F	-57.9	-72.2
WF-70 (WOG), -35 °F	-54.4	-65.9
WF-70 (WOG), -70 °F	-53.2	-63.8
Mean	-55.2	-67.3
Standard Deviation	2.4	4.4
WF-70 BAW-2202 (1993)		
WF-70 (BAW-2202), 0 °F	-32.6	-26.7

Table 4-4 Reference Temperatures for Linde 80 Welds - 1995 Test Data and ORNL HSST Data

Weld Metal	T_o, C	T_o, F
WF-25	-68.8	-91.8
SA-1526	-75.5	-103.9
WF-193	-84.1	-119.4
WF-182-1	-80.3	-112.5
WF-112	-91.1	-132.0
ORNL 63W, -75 F	-73.1	-99.6
ORNL 64W, -58 F	-61.6	-78.9
ORNL 65W, -94 F	-82.0	-115.6
Mean	-77.1	-106.7
Standard Deviation	9.3	16.8

Figure 4-1 Comparison of Three Master Curves for WF-70 at Three Test Temperatures

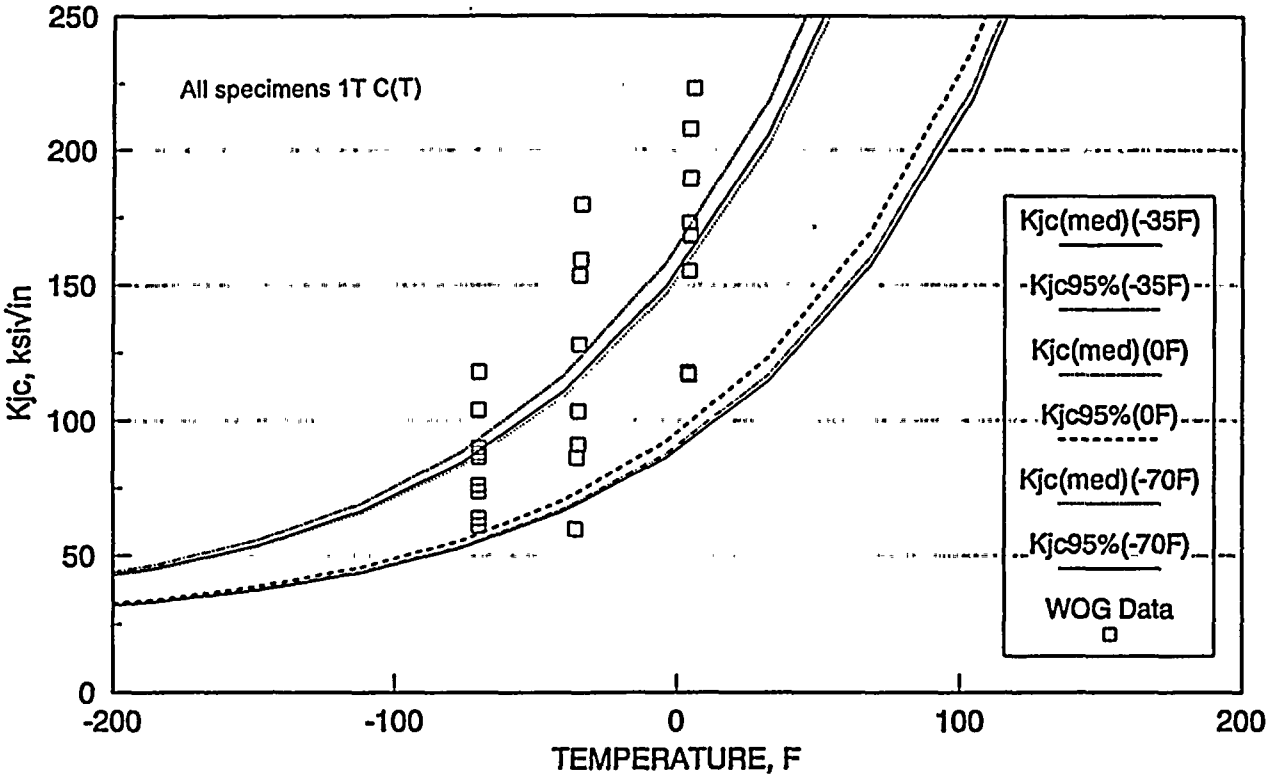

Figure 4-2 WF-70 Fracture Toughness - Specimen Size Effect

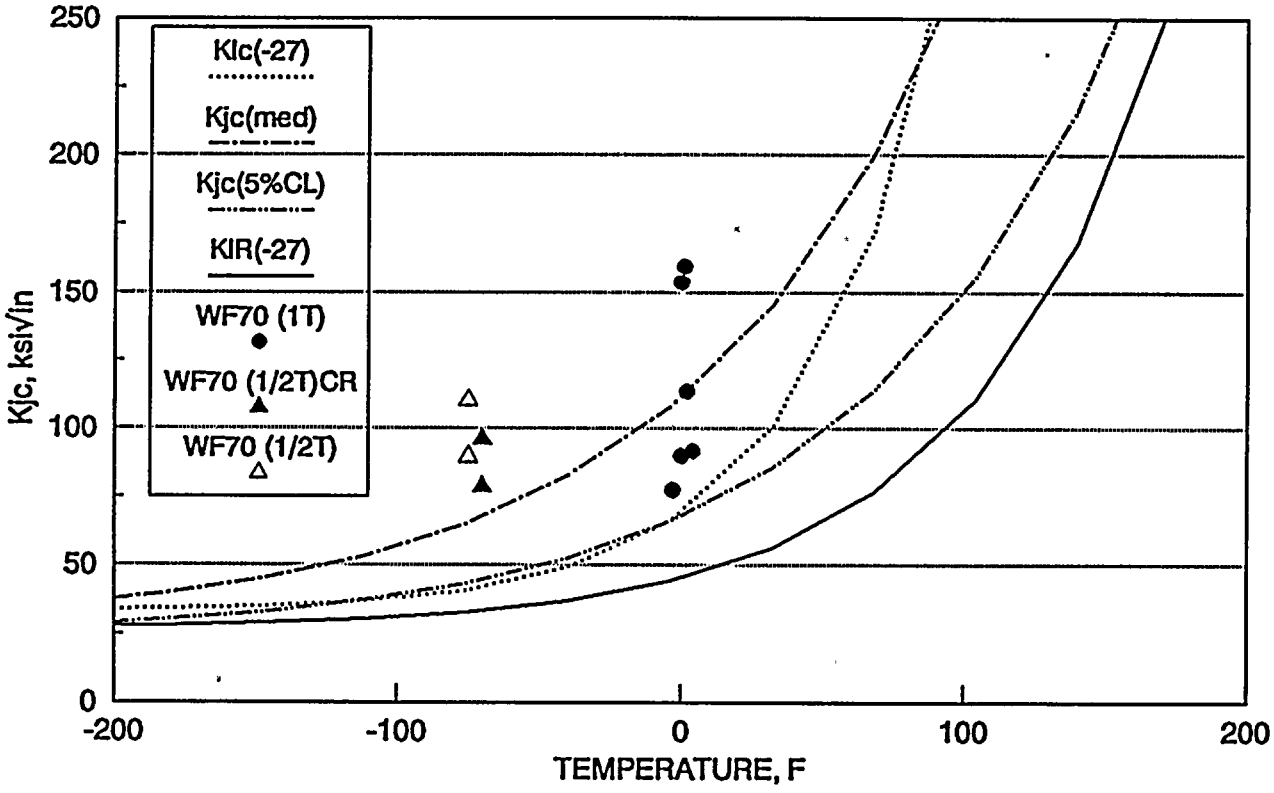

Figure 4-3 Fracture Toughness Data for Six Linde 80 Weld Metals

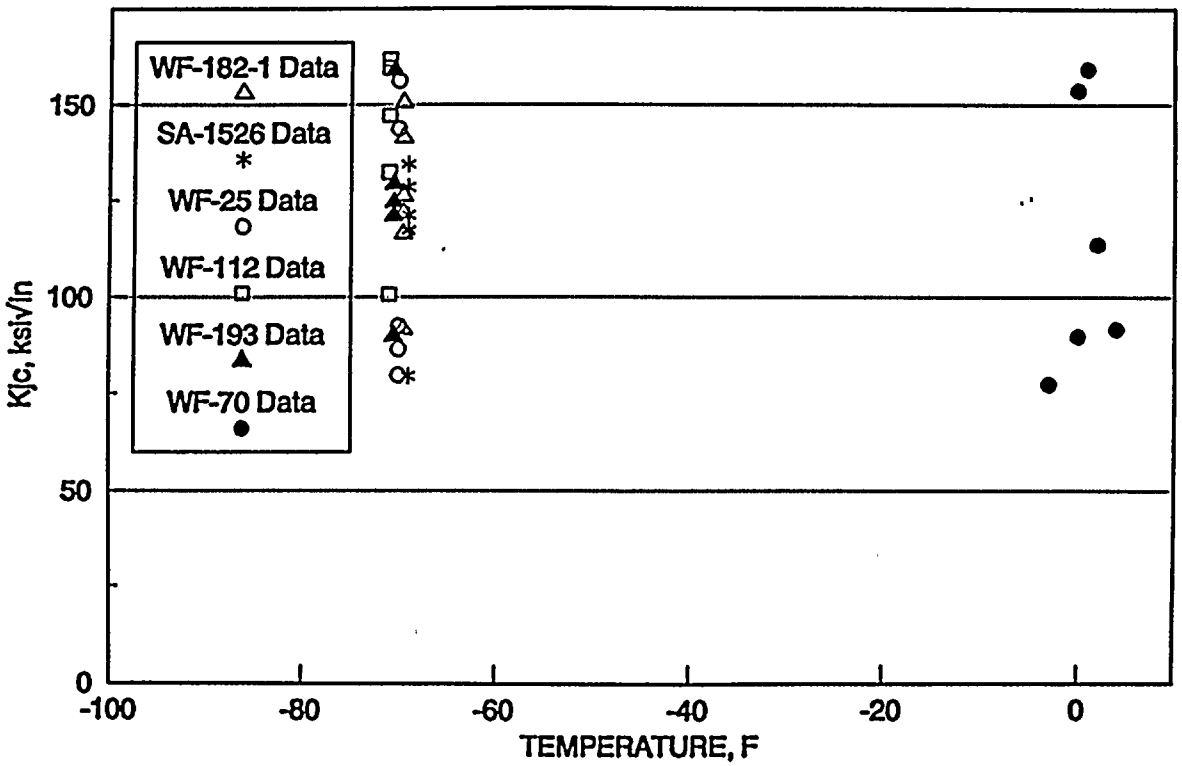

Figure 4-4 Weibull Plot for WF-25 Data

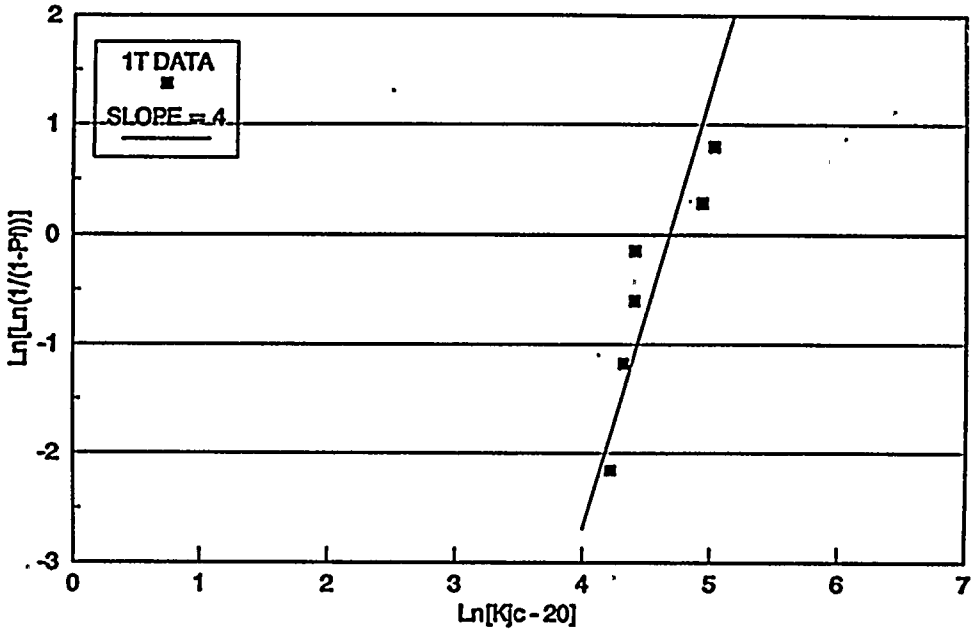

Figure 4-5 Fracture Toughness Comparison - Static Toughness Data of WF-25

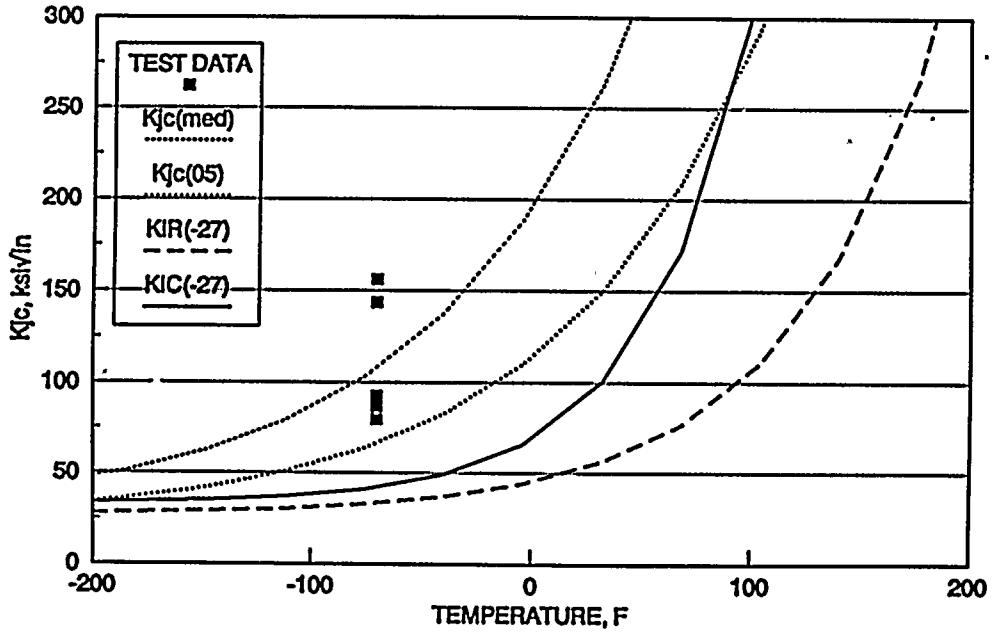

Figure 4-6 Weibull Plot for SA-1526 Data

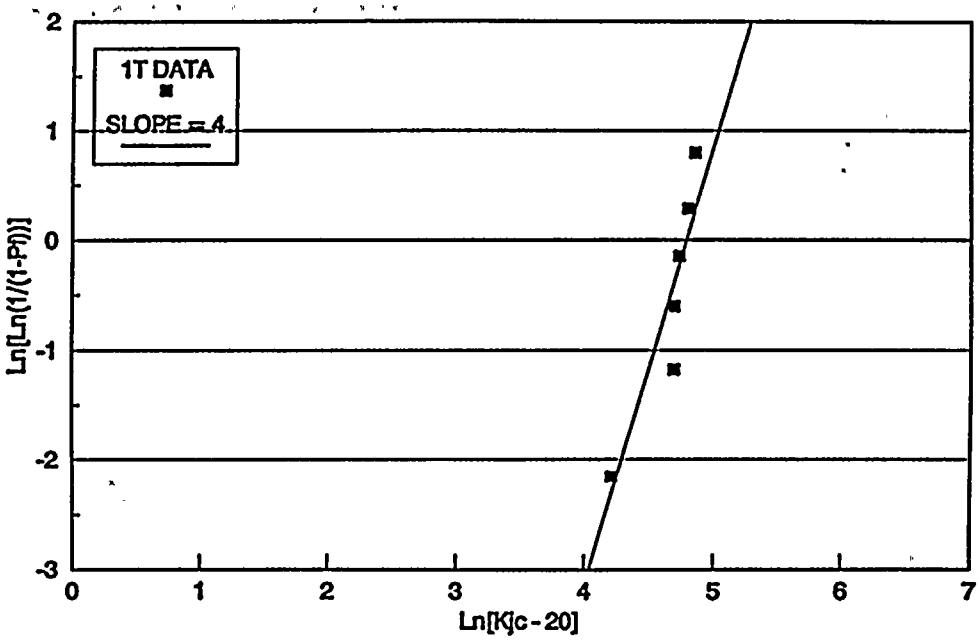

Figure 4-7 Fracture Toughness Comparison - Static Toughness Data of SA-1526

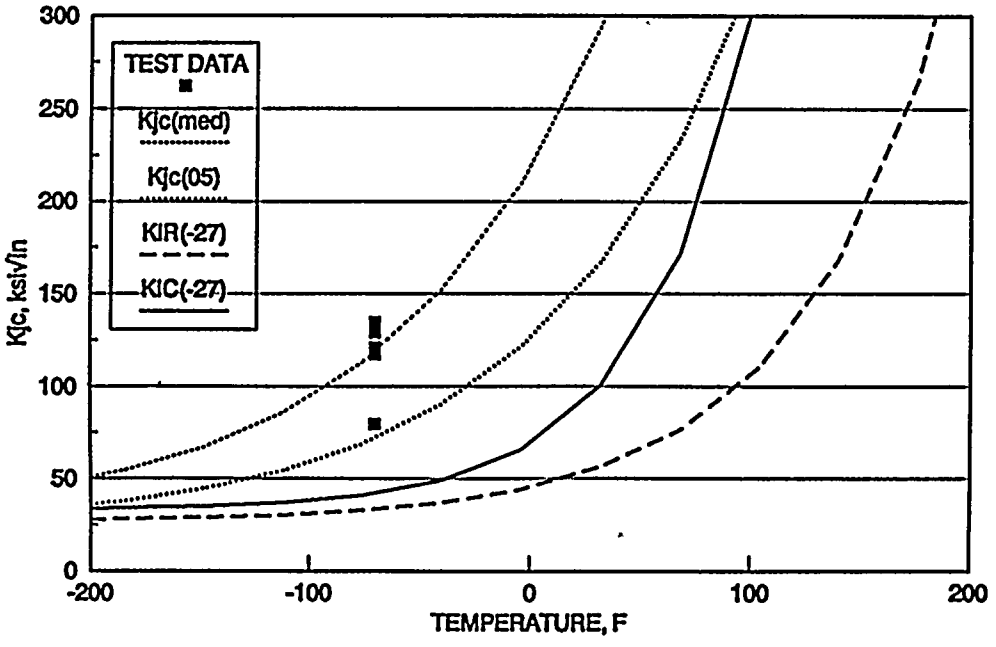

Figure 4-8 Weibull Plot for WF-193 Data

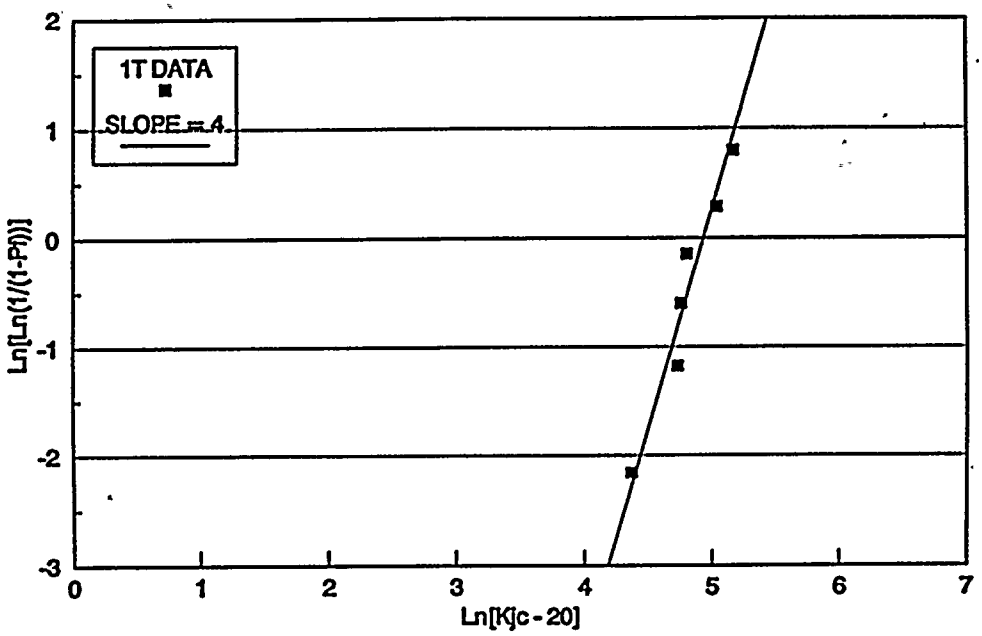

Figure 4-9 Fracture Toughness Comparison - Static Toughness Data of WF-193

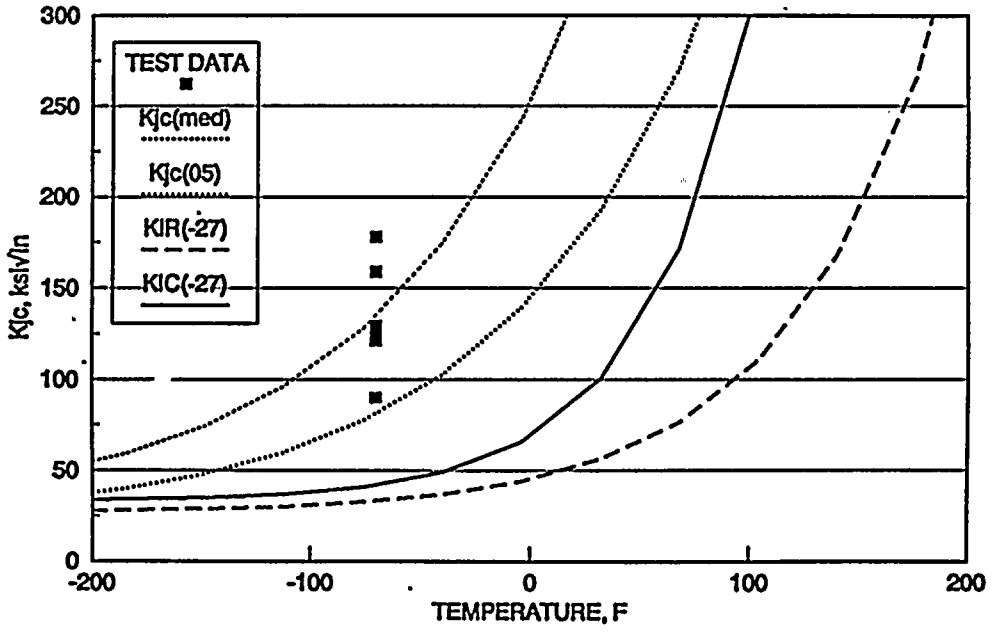

Figure 4-10 Weibull Plot for WF-182-1 Data

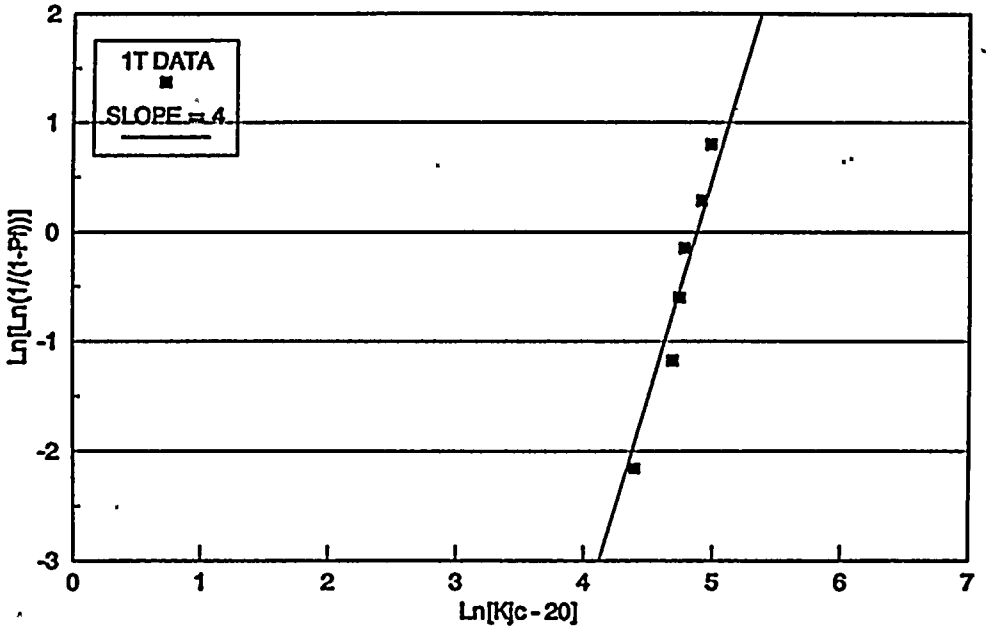

Figure 4-11 Fracture Toughness Comparison - Static Toughness Data of WF-182-1

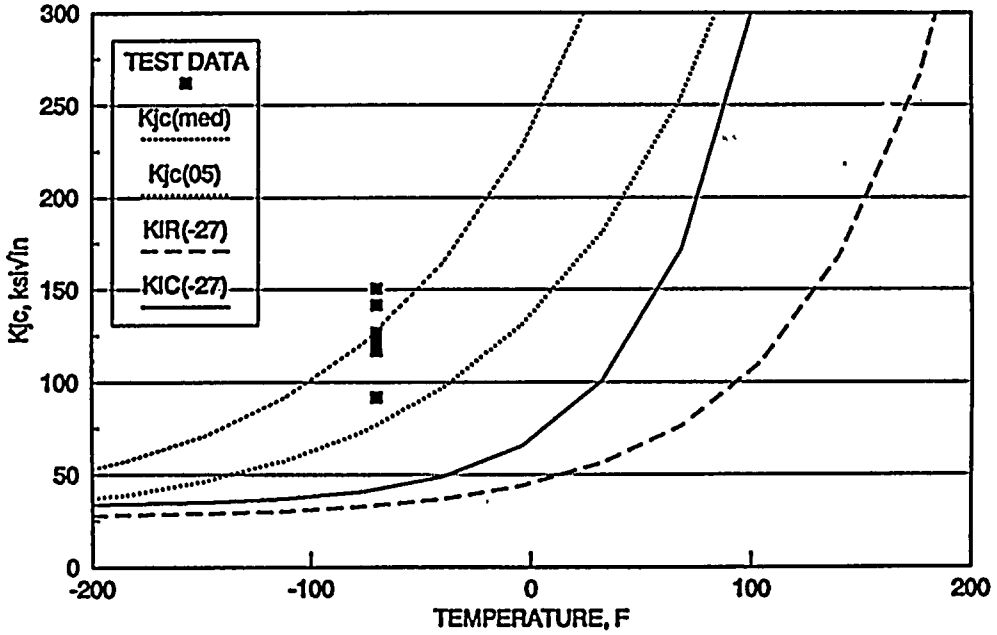

Figure 4-12 Weibull Plot for WF-112 Data

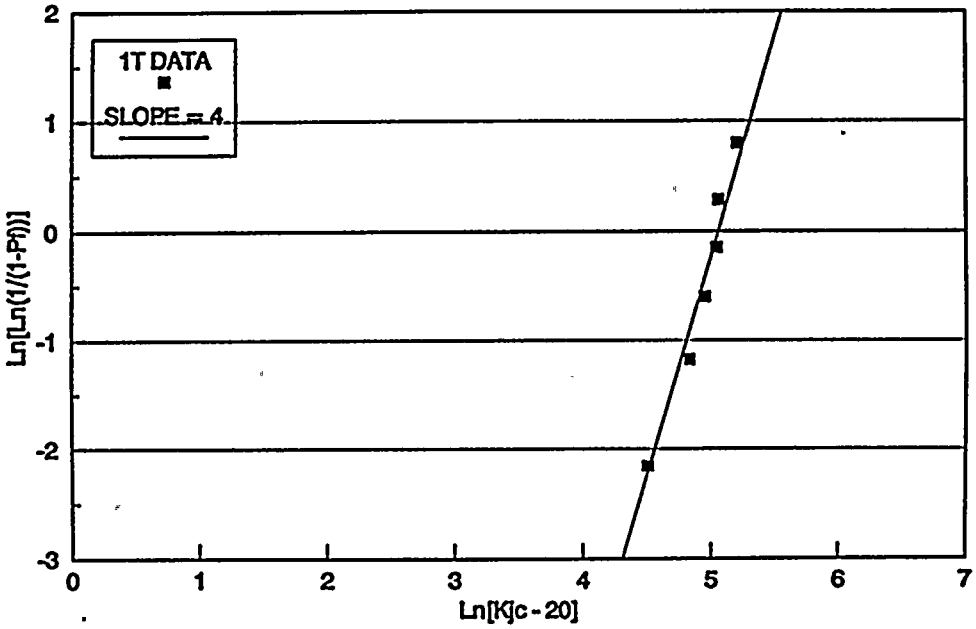

Figure 4-13 Fracture Toughness Comparison - Static Toughness Data of WF-112

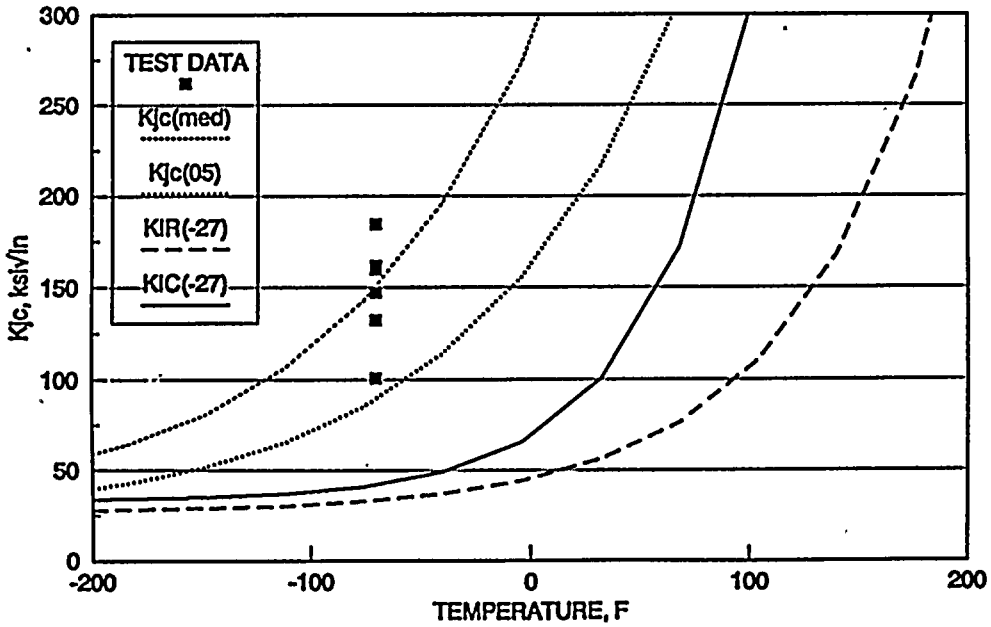

5. ALTERNATIVE IRT_{NDT} BY FRACTURE TOUGHNESS

The data analysis described in Section 4 resulted in five master curves. These additional master curves are compared with the WF-70 master curve to establish an IRT_{NDT} for the family of Linde 80 weld metal family. The IRT_{NDT} value for WF-70 was established by the submittal of BAW-2202.

5.1. Comparison of Master Curves of Linde 80 Welds

Figure 5-1 shows the new static fracture toughness data plotted with the WF-70 master curve and data at 0 F. The additional fracture toughness data at -70 F have generally higher values than the WF-70 data at 0 F. These new data show higher toughness than the WF-70. As discussed in Paragraph 4.5., the reference temperature determines the relative shift of the median Kjc curves. The highest reference temperature seen from the new data set is -68.8 C (-91.8 F) for WF-25. All the other materials have lower values, as shown in Table 4-3. Compared to these values, the reference temperature for WF-70 was -32.6 C (-26.7 F). That is, the toughness of all additional Linde 80 weld is bounded by the WF-70 master curve as demonstrated in Figure 5-2.

5.2. Comparison of Static Fracture Toughness with Additional Data

Recently, ORNL analyzed Linde 80 (63W, 64W, and 65W) fracture toughness data[10] in the HSST Series 2. The master curves from this analysis is shown in Figure 5-3 and are compared with the WF-70 curves. This supports the findings of the RVWG additional data analysis showing that the WF-70 master curve lower bounds all other Linde 80 master curves. A comparison of the reference temperature in Table 4-3 indicates that the difference among the mean reference temperature value is only approximately 8 C (14.4 F).

Figure 5-1 Fracture Toughness Curves and All Linde 80 Weld Metal Data

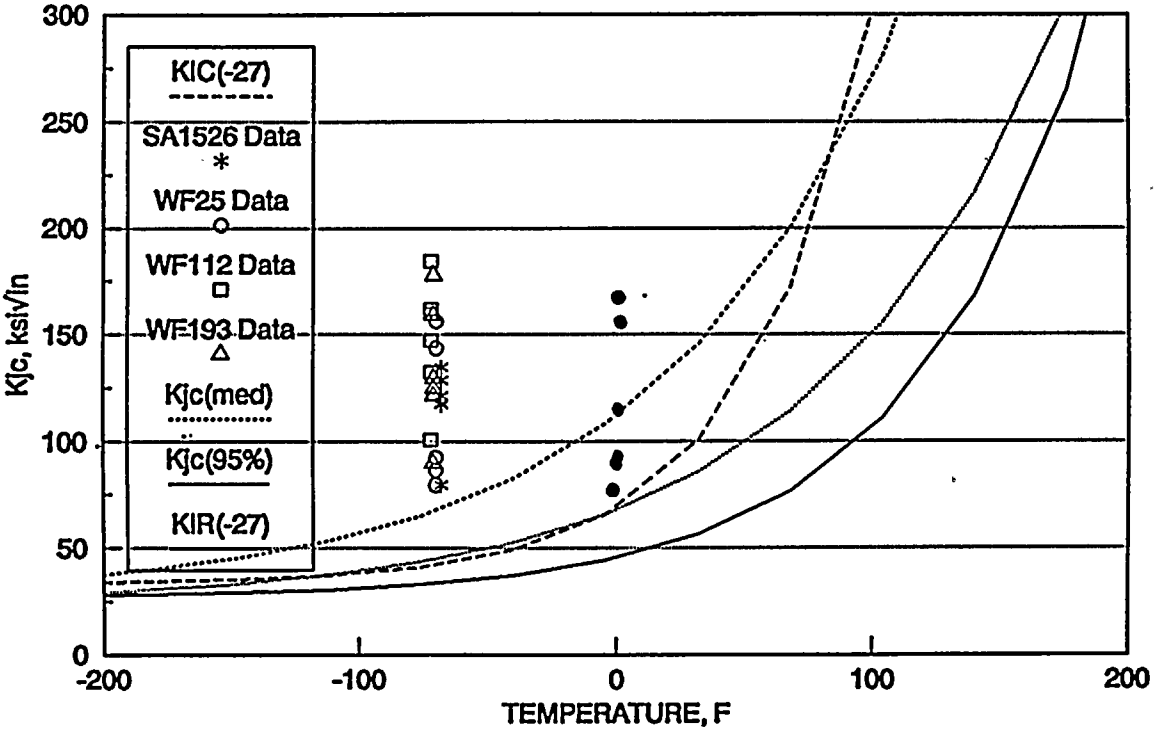

Figure 5-2 Master Curves - B&WOG Linde 80 Weld Metal Data

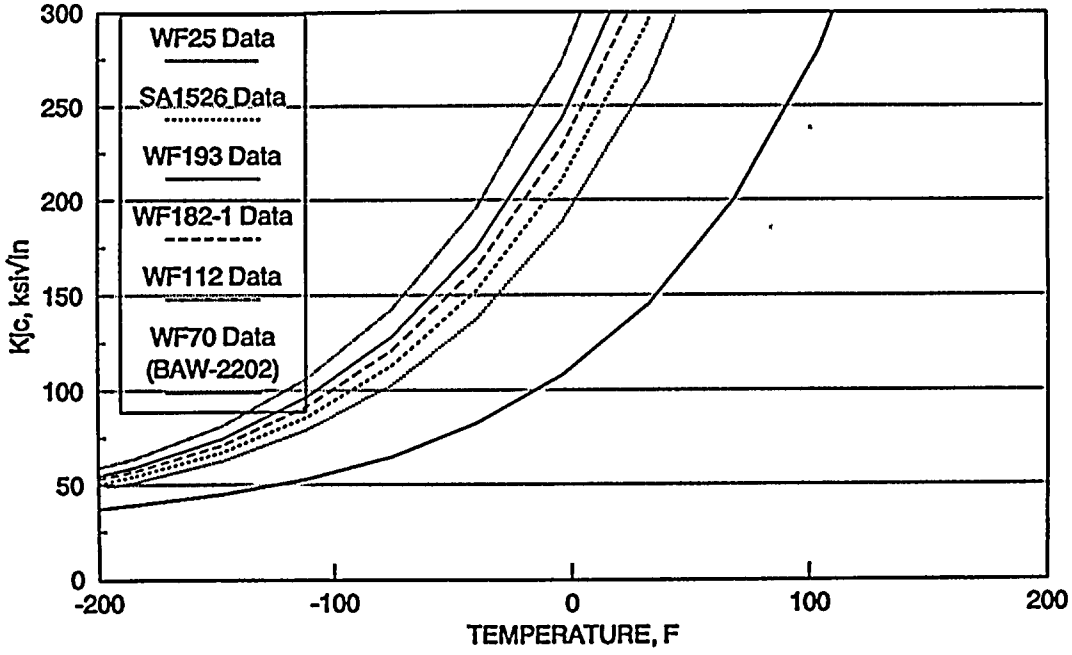

Figure 5-3 Master Curves - ORNL Linde 80 Weld Metal Data

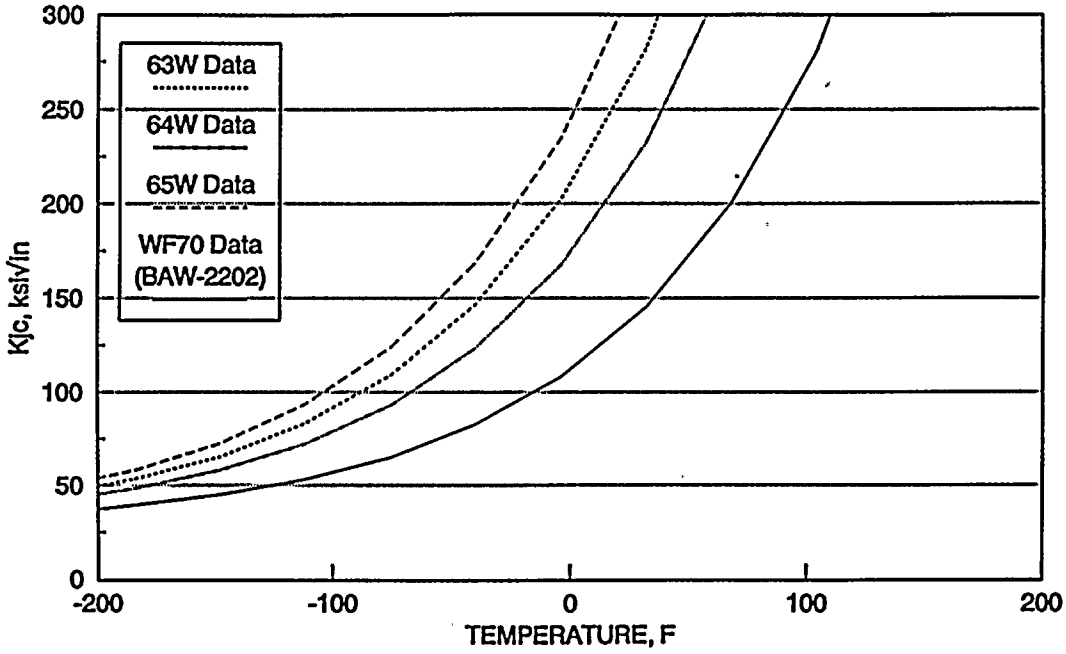

6. CONCLUSIONS

Following a successful application of the alternative method of determining initial RT_{NDT} to the WF-70 weld metal, the RVWG expanded the transition data base to include additional Linde 80 welds. Additional data analysis using the master curve method yielded a basis to compare the fracture toughness of a number of Linde 80 welds to WF-70. The following conclusions are drawn from this effort:

1. Linde 80 weld material master curves are very close to each other.
2. These master curves are all bounded by the WF-70 curve, therefore, the WF-70 IRT_{NDT} value of -27 F can be applied to other Linde 80 welds.
3. Comparisons made with ORNL Linde 80 weld data also indicate that the proposed IRT_{NDT} of -27 F if applied to all Linde 80 welds is conservative.

7. REFERENCES

1. K. K. Yoon, "Fracture Toughness Characterization of WF-70 Weld Metal," BAW-2202, B&W Nuclear Technologies, Lynchburg, Virginia, September 1993.

2. L. B. Gross, "Chemical Composition of B&W Fabricated Reactor Vessel Beltline Welds," BAW-2121P, B&W Nuclear Technologies, Lynchburg, Virginia, April 1991.

3. L. S. Harbison, "Master Integrated Reactor Vessel Surveillance Program," BAW-1543, Rev. 4, B&W Nuclear Technologies, Lynchburg, Virginia, February 1993.

4. M. J. DeVan, "Evaluation of Tension Test Data for Reactor Vessel Beltline Materials," BAW-2240P, B&W Nuclear Technologies, Lynchburg, Virginia, December 1994.

5. Code of Federal Regulation, Title 10, Part 50, Paragraph 61, "Fracture Toughness Requirements for Protection Against Pressurized Thermal Shock Events."

6. U. S. Nuclear Regulatory Commission, "Radiation Embrittlement Damage to Reactor Vessel Materials," Regulatory Guide 1.99, Revision 2, May 1988.

7. "PVRC Recommendation on Toughness Requirements for Ferritic Materials," WRC Bulletin 175, Welding Research Council, New York, August 1972.

8. R. K. Nanstad, D. E. McCabe, R. L. Swain, and M. K. Miller, "Chemical Composition and RT_{NDT} Determinations for Midland Weld WF-70," NUREG/CR-5914, U. S. Nuclear Regulatory Commission, Washington, D.C., December 1992.

9. A. Begley, "Effects of Section Size and Cleanliness on the Upper-shelf and Transition Range Toughness of Three Nuclear Pressure Vessel Steels, " WOG-93-013 Westinghouse Owners Group, January 23, 1993.

10. A. Sokolov, et al., "HSSI Program Includes Annealing and Reirradiation of High-Copper, Low Upper-Shelf Welds," ORNL, BWOG/ORNL/USNRC Meeting, Knoxville, Tennessee, March 23.

8. CERTIFICATION

This report is an accurate description of the fracture toughness characterization of Linde 80 weld metals and the results are accurately reported. The conclusions described are based on the data analysis presented.

K. K. Yoon — Oct. 9, 95
K. K. Yoon — Date
Materials and Structural Analysis

This report was reviewed and was found to be an accurate description of the work reported.

A. D. Nana — Oct. 9 '95
A. D. Nana — Date
Materials and Structural Analysis

Verification of independent review.

K. E. Moore — Oct. 9, 95
K. E. Moore, Manager — Date
Materials and Structural Analysis Unit

This report has been approved for release.

D. L. Howell — Oct 13, '95
D. L. Howell, Program Manager — Date
B&W Owners Group - RV Integrity Program

Appendix A

ASTM E08.08 Subcommittee on Elastic Plastic Fracture Mechanics Technology

Draft No.10, "Test Practice (Method) for Fracture Toughness in the Transition Range"

DRAFT 10 Rev. 6-12-95

TEST PRACTICE (METHOD) FOR FRACTURE TOUGHNESS IN THE TRANSITION RANGE

CONTENTS

TEST PRACTICE (METHOD) FOR FRACTURE TOUGHNESS IN THE TRANSITION RANGE

1. SCOPE

1.1 This practice covers the determination of fracture toughness for ferritic steels that experience onset of cleavage cracking at elastic, and/or elastic-plastic K_{Jc} instabilities. The specific types of ferritic steels covered are those of yield strength ranging from 275 to 825 MPa (40 to 120 ksi) and weld metals that have been stress-relief annealed or that have <10% strength mismatch to that of the base metal. The specimens covered are fatigue precracked single-edge notched bend bars, SE(B), and standard or disk-shaped compact specimens, C(T) or DC(T).

1.2 A range of specimen sizes with proportional dimensions is recommended. The basis dimension for the proportionality is specimen thickness.

1.3 Requirements are set on specimen size and the number of replicate tests that are needed to establish acceptable characterization of K_{Jc} data populations.

1.4 Size effects on K_{Jc} toughness are predicted using the theory of weakest-link statistics. Limits are set on the range of applicability.

1.5 K_{Jc} transition temperature curves are predicted using statistical methods. Standard deviation of data distribution is a function of Weibull slope and median K_{Jc}. The procedure for applying this information to the establishment of transition temperature shift determinations and the establishment of confidence limits is prescribed.

2. REFERENCED DOCUMENTS

2.1 ASTM Standards

E4 - Standard Practices for Load Verification of Testing Machines

E8 - Standard Test Methods of Tension Testing of Metallic Materials

E74 - Standard Practice of Calibration of Force-Measuring Instruments for Verifying the Force Indication of Testing Machines

E399 - Standard Test Method for Plane-Strain Fracture Toughness of Metallic Materials

E561 - Standard Practice for R-Curve Determination

E616 - Standard Terminology Relating to Fracture Testing

E812 - Standard Test Method for Crack Strength of Slow-Bend Precracked Charpy Specimens of High-Strength Metallic Materials

E813 - Standard Test Method for J_{Ic}, A Measure of Fracture Toughness

E1152 - Standard Test Method for Determining J-R Curves

3. SUMMARY OF TEST METHOD

3.1 This method involves the testing of notched and fatigue precracked bend or compact specimens in a temperature range where cleavage cracking and/or crack pop-in develops during the loading of specimens. Crack aspect ratio, a/W, is nominally 0.5. Specimen width in compact specimens is two times the thickness. In bend bars, specimen width can be either one or two times the thickness.

3.2 Load versus displacement across the notch at a specified location is recorded by autographic recorder and/or computer data acquisition. Fracture toughness is calculated at a defined condition of crack instability. J-integral at instability, J_c, is calculated and converted into its equivalent in units of stress intensity factor, K_{Jc}. Limits are set on the suitability of data for data population analyses.

3.3 Tests that are replicated at least six times can be used to establish the Weibull distribution for the data population. Extensive data scatter among replicate tests is expected. Statistical methods are used to characterize these data populations and to make predictions of how data populations change with specimen size.

3.4 The relationship between specimen size and K_{Jc} fracture toughness can be estimated using weakest-link theory.[1] Limits are placed on the fracture toughness range over which this model can be used.

3.5 For definition of the toughness transition curve, a master curve concept is used.[2] The position of the curve on the temperature coordinate is established from the experimental determination of the temperature at which the median K_{Jc} for 1T size specimens is 100 MPa$\sqrt{m}$ (90.9 ksi$\sqrt{in.}$). This temperature, designated T_o, may be used to quantify degradation of fracture toughness due to embrittlement mechanisms. Selection of a test temperature close to that at which the median K_{Jc} value will be 100 MPa$\sqrt{m}$ is encouraged and a means of estimating this temperature is suggested.

3.6 Confidence band limits can be determined that define the range of data scatter throughout the transition range. Data scatter is a function of Weibull slope and median K_{Jc} value, $K_{Jc(med)}$.

4. SIGNIFICANCE AND USE

4.1 Fracture toughness is expressed in terms of an elastic-plastic stress intensity factor, K_{Jc}, that is calculated from J integral at fracture.

4.2 Distributions of K_{Jc} data from replicate tests can be used to predict distributions of K_{Jc} for different specimen sizes. Standard deviation on data scatter can be calculated. Data distribution and specimen size effects on median toughness are characterized using a Weibull function and weakest-link statistics.[3] A window of applicability is defined where weakest-link statistics can be used. The upper and lower limits on this window are established through constraint/toughness parameters.

4.3 A master curve is defined that describes the shape and location of median K_{Jc} transition temperature fracture toughness for 1T specimens.[4] The curve is positioned on the abscissa (temperature coordinate) by an experimentally determined reference temperature, T_o. Shifts in reference temperature are a measure of transition temperature change from metallurgical damage mechanisms.

4.4 Confidence limits on K_{Jc} are calculated based on theory and generic data. For added conservatism, an offset can be added to confidence limits to cover the uncertainty associated with estimating the reference temperature, T_o, from a relatively small data set. From this it is possible to apply a margin adjustment to T_o in the form of a reference temperature shift.

5. TERMINOLOGY

5.1 Terminology given in E 616 is applicable to this standard.

5.2 Definitions

5.2.1 Stress intensity factor, $K[FL^{-3/2}]$ - The magnitude of the ideal linear elastic singular term crack tip stress field coefficient for a particular mode of crack tip region deformation in a homogeneous body. Discussion: In this method, mode I is assumed.

5.2.2 J-integral, $J[FL^{-1}]$ - A mathematical expression, an integral over a line or surface enclosing the crack front from one crack surface to the other; used to characterize the local stress-strain field around the crack front.[5] See E616 for further discussion.

5.2.3 Elastic-plastic $K_{Jc}[FL^{-3/2}]$ - An elastic-plastic equivalent stress intensity factor derived from the J-integral at the point of onset of cleavage fracture, J_c.

5.2.4 Yield strength, $\sigma_{ys}[FL^{-2}]$ - A value of material strength at 0.2% plastic strain as determined in tensile tests.

5.2.5 Elastic modulus, $E'[FL^{-2}]$ - A linear-elastic stress-strain ratio, the value of which is dependent on the degree of constraint. For plane strain, $E' = E/(1 - \nu^2)$ is used and for plane stress $E' = E$. Discussion: In this method, plane stress elastic modulus is used.

5.2.6 Effective modulus, $E_e[FL^{-2}]$ - An elastic modulus that can be used with experimentally determined elastic compliance to affect an exact match to theoretical (modulus normalized) compliance for the actual crack size, a_o.

5.2.7 Control load, $P_M[F]$ - A calculated value of maximum load used in E1152 to stipulate allowable precracking limits. Discussion: In this method, P_M is not used for precracking, but is used as a minimum load above which partial unloading is started for crack growth measurement.

5.2.8 Specimen thickness, B[L] - The distance between the sides of specimens. Discussion: In the case of side-grooved specimens, thickness, B_N, is the distance between the roots of the side-groove notches.

5.2.9 Initial ligament length, b_o [L] - The distance from the initial crack tip to the back face of a specimen.

5.2.10 Physical crack size, a[L] - The distance from a reference plane to the observed crack front. The reference plane depends on the specimen form. Normally it is taken to be either the plane containing the load line or the front face of the specimen. For compact specimens, it is the load-line and for bend specimens it is the front face.

5.2.11 SE(B) specimen span, S[L] - The distance between specimen supports (see E1152, Fig. 2).

5.2.12 Pop-in - A discontinuity in a load versus displacement test record.[6] A pop-in event is usually audible, and is a sudden cleavage crack initiation event followed by crack arrest. A test record will show increased displacement and drop in applied load if the test frame is stiff. Subsequently, the test record continues on to higher loads and increased displacement.

5.2.13 Eta (η) - A dimensionless parameter that relates total work done on a specimen to crack growth resistance defined in terms of deformation theory J-integral.[7]

5.2.14 Specimen size, nT - A code used to define specimen dimensions, where n is expressed in multiples of 1 in. Discussion: In this practice, specimen proportionality is required; for compact specimens and bend bars. Specimen thickness B = n inches.

5.2.15 Failure probability, P_f - The probability that a single selected specimen chosen from a population of specimens will fail at or before reaching the K_{Jc} value of interest.

5.2.16 Weibull fitting parameter, K_0 - A scale parameter located at the 63.2% cumulative failure probability level.[8] $K_0 = K_{Jc}$ when $P_f = 0.632$.

5.2.17 Weibull slope, b - With P_f and K_{Jc} data pairs plotted in Weibull coordinates (see Figs. A1 and B1), b is the slope of a line that defines the typical data scatter characteristics of K_{Jc} data. Discussion: A Weibull slope of 4 is used exclusively in this practice.

5.2.18 Reference temperature, T_o [°C] - The test temperature where the median of the K_{Jc} distribution from 1T size specimens will equal 100 MPa√m (90.9 ksi√in.).

6. APPARATUS

6.1 Precision of instrumentation - Measurements of applied loads and load-line displacements are needed to obtain work done on the specimen. Load versus load-line displacements may be recorded digitally on computers or autographically on x-y plotters. For computers, digital signal resolution should be 1/32,000 of the transducer signal range and 1/4000 of the load transducer signal range.

6.2 Grips for C(T) specimens - A clevis with flat-bottom holes is recommended. See E399, Fig. A6.2, for a recommended design. Clevises and pins should be fabricated from steels of sufficient strength to elastically resist indentation loads [greater than 40 Rockwell hardness "C" scale (HRC)].

6.3 Bend test fixture - A suitable bend test fixture scheme is shown in Fig. A3.2 of E 399. It allows for roller pin rotation and minimizes friction effects during the test. Fixturing and rolls should be made of high-hardness steel (greater than 40 HRC) steels.

6.4 Displacement Gage for Compact Specimens

6.4.1 Displacement measurements are needed to evaluate J from area under load versus displacement test records (a measure of work done). If the test temperature selection recommendations of this practice are followed, crack growth measurement will probably prove to be unimportant. Test data that fall within the limits of uncertainty of the recommended test temperature estimation scheme will probably not have significant slow-stable crack growth prior to instability. Nevertheless, crack growth measurements are recommended to provide supplementary information, and these results shall be reported.

6.4.2 To measure slow-stable crack growth, unloading compliance is the primary recommendation. See method E1152. When multiple tests are performed sequentially at low test temperatures, there will be condensation on the grips and consequently there will be a tendency for ice buildup between the loading pins and flats of the clevis holes. Ice will interfere with the accuracy of the unloading compliance method. Alternatively, crack growth can be measured

by other methods such as electric potential, but care must be taken to avoid specimen heating when low test temperatures are used.

6.4.3 In compact C(T) specimens, displacement measurements on the load line are recommended to determine J. However, the front face position at 0.25 W in front of the load line can be used with interpolation to load-line displacement, as suggested in 7.1.

6.4.4 The extensometer calibrator shall be resettable at each displacement interval within 0.0051 mm (0.0002 in.). Accuracy of the clip gage at test temperature must be demonstrated to be within 1% of the working range of the gage.

6.4.5 All clip gages used shall have temperature compensation.

6.5 Displacement Gages for Bend Bars, SE(B)

6.5.1 The SE(B) specimen has two displacement gage locations. A load-line displacement transducer is primarily intended for J computation, but may also be used for elastic compliance calculations of crack size, if provision is made to subtract the extra displacement due to the elastic compliance of the fixturing. The load-line gage shall display accuracy of 1% over the working range of the gage. The gages used shall not be temperature sensitive.

6.5.2 A crack mouth opening displacement (CMOD) gage can also be used to determined J. However, it is necessary to employ a plastic eta (ηp) value developed specifically for that position[9] or infer load point displacement from mouth opening using an expression that relates the two displacements.[10] In either case, the procedure described in 9.1.3 is used to calculate J. The CMOD position is the most accurate for the determination of slow-stable crack growth.

6.5.3 Crack growth can be measured by alternative methods such as electric potential, but care must be taken to minimize specimen heating effects in low-temperature tests.

6.6 Load Transducers

6.6.1 Testing shall be performed in a machine conforming to the practices of E4. Applied load may be measured by any load transducer capable of constant and steady output.

6.6.2 Calibrate load cells via ASTM Standard Practice E74-83, 10.2. Annual calibration using calibration equipment traceable to the National Institute of Standards and Technology is a mandatory requirement.

6.7 Temperature control - Temperature shall be measured with calibrated thermocouples and potentiometers. Accuracy of temperature measurement shall be within 3°C of true temperature and repeatability shall be within 2°C. Precision of measurement shall be ±1°C or better. The temperature measuring apparatus shall be checked every 6 months using instruments traceable to the National Institute of Standards and Technology in order to ensure the required accuracy.

7. SPECIMEN CONFIGURATION, DIMENSIONS AND PREPARATION

7.1 Compact specimens - Three recommended C(T) specimen designs are shown in Fig. 1. One C(T) specimen configuration is taken from Standard Test Method E399, and the other two with cutout sections are taken from E1152. The latter two designs are modified to permit load line displacement measurement. Room is provided for attachment of razor blade tips on the load line. Care should be taken to maintain parallel alignment of the blades. When front face (at 0.25W in front of the load line) displacement measurements are made with the E399 design, the load-line displacement is inferred by multiplying the measured values by the constant 0.73.[11] The ratio of specimen height to width, 2H/W is 1.2, and this ratio is to be the same for C(T) specimens of all types and sizes. The initial crack size, a_o, shall be 0.5W ± 0.05W. Specimen width, W, shall be 2B.

7.2 Disk-shaped compact specimens - A recommended DC(T) specimen design is shown in Fig. 2. Initial crack size, a_o, shall be 0.5W ± 0.05W. Specimen width shall be 2B.

7.3 Single edge notched bend - The recommended SE(B) specimen designs, shown in Fig. 3, have a span-to-width ratio, S/W = 4. The width, W, can be either 1B or 2B. The initial crack size, a_o, shall be 0.5W ± 0.05W.

7.4 Machined notch design - The machined notch plus fatigue crack for all specimens shall lie within the envelope shown in Fig. 4.

7.5 Specimen dimension requirements - For the data to be valid by this method, the specimen initial remaining ligament, b_o, must satisfy the size requirement given in 10.2.2, and the crack front straightness must satisfy the criterion of 8.8.1.

7.5.1 K_{Jc} data can be used to predict size effects provided sufficient constraint exists at the onset of cleavage fracture. Constraint loss is limited through the use of the following fracture toughness limitiation:

$$K_{Jc} \leq (Eb_o\sigma_{ys}/30)^{1/2}. \quad (1)$$

For the recommended specimen configurations, a K_{Jc} toughness value can be used in statistical model definition (including size effect predictions) when the K_{Jc} value for that specimen is less than or equal to the value set by the right hand side of Eq. (1).

7.6 Side grooves - Side grooves are optional. Specimens may be side grooved to ensure a straight initial crack front. The total side grooved depth shall not exceed 0.25B. Side grooves with an included angle of 45° and a root radius of 0.5 ± 0.2 mm (0.02 ± 0.01 in.) usually produce the desired results.

7.7 Precracking specimens - All specimens shall be precracked in the final heat treated condition. If the progress of crack growth is to be followed visually, side grooving prior to precracking is not recommended. The length of the fatigue precrack extension shall not be less than 5% of the total crack size. Precracking may include two stages: crack initiation and finish sharpening of the crack tip. To avoid growth retardation from a single unloading step, intermediate levels of load shedding can be added if desired. To initiate fatigue crack growth from a machined notch, use $K_{max}/E = 0.00013\ m^{1/2}$ ($0.00083\ in.^{1/2}$) ± 5%.[Note 1] Stress ratio, R, shall be controlled within the following range: $0.01 < R < 0.1$. Finish sharpening is to be started at least 0.6 mm (0.025 in.) before the end of precracking. K_{max}/E for finish sharpening is to be $0.000096\ m^{1/2}$ ($0.0006\ in.^{1/2}$) ± 5% and stress ratio shall be maintained in the range $0.01 < R < 0.1$. If the test material is a ferritic steel, or a heat treated grade of steel, and the precracking temperature, T1, is different than

---

[Note 1] Elastic (Young's) modulus, E, in units of ksi will yield K_{max} in units of ksi√in. Elastic (Young's) modulus, E, in units of MPa will yield K_{max} in units of MPa√m.

the test temperature, T2, then the finish sharpening K_{max}/E shall be equal to or less than $[\sigma_{ys(T1)}/\sigma_{ys(T2)}]$ 0.000096 $m^{1/2}$ ± 5%. The lowest practical stress ratio is suggested in all cases. Finish sharpening can be expected to require between 5×10^3 to 5×10^5 cycles for most metallic test materials when using the above recommended K levels. If the material being prepared does not precrack using the above recommended K_{max} requirements, variance is allowed only if it is shown that K_{max} does not exceed 60% of the K_{Jc} value obtained in the subsequent test. Finish sharpening shall not take less than 10^3 cycles to produce the last 0.6 mm of growth.

8. PROCEDURE

8.1 Testing procedure - The objective of the procedure described here is to determine the J-integral at the point of crack instability, J_c. Crack growth can be measured by partial unloading compliance, or by any other method that has reasonable precision and accuracy, as defined below. J-integral is not corrected for slow-stable crack growth in this practice, however.

8.2 Preparation for tests - Prior to each test, certain specimen dimensions should be measured, the clip gage checked, and the starting crack size estimated.

8.2.1 The dimensions B, B_N, and W shall be measured to within 0.05 mm (0.002 in.) accuracy or 0.5%, whichever is larger. Initial crack size is to be calculated, based on the average of the two visual measurements on the specimen side faces, after precracking.

8.2.2 Because most tests conducted under this practice will terminate in specimen instability, clip gages tend to be abused, and they shall be examined for damage after each test and checked electronically before each test. Clip gages shall be calibrated at the beginning of each day of use, using an extensometer calibrator or other suitable device of equal or better sensitivity. See also 6.4.4.

8.3 Preparation for testing - Follow ASTM Standard Test Method E1152-87, 8.2.3 to set up compact specimen tests and 8.2.4 to set up bend specimens.

8.4 Test temperature selection - This practice recommends the selection of a test temperature close to that at which the mean of K_{Jc} values will be about 100 MPa√m. Charpy V-notch data, preferably for the T-L orientation, can be used as an aid to predict a viable test temperature. Determine the temperature for a Charpy V-notch energy of 28 J, T_{28J}. Estimate test temperature, T, using the following:[12]

$$T = T_{28J} + C \, . \qquad (2)$$

Units of the constant C are in degrees Celsius and C is a function of specimen size, nT (defined in 5.2.13) as follows:[Note 2]

Specimen size (nT)	Constant, C (°C)
0.4T	–32
0.5T	–28
1T	–18
2T	–8
3T	–1
4T	2

Despite the large scatter in the estimate on T [Eq. (2)], the likelihood of slow-stable crack growth prior to onset of cleavage fracture will be low. Also, all specimens of the material sample are likely to provide valid K_{Jc} data.[Note 3]

8.5 Specimen test temperature control and measurement - For tests at temperatures other than ambient, any suitable means (liquid, gas vapor, or radiant heat) may be used to cool or heat the specimens, provided the region near the crack tip can be maintained at the desired temperature within ±2°C (4°F) during the soak period and during the conduct of the test.

8.5.1 Temperature shall be measured by a thermocouple attached to the specimen near the crack tip but not directly on the plane of crack propagation. The attachment method can be by spot weld, drilled hole, or by a firm mechanical holding device so long as these practices do not disturb the crack tip stress field of the specimen during loading. Temperature of the specimen shall be measured until the specimen reaches test temperature and soaks at the test temperature for 5 minutes per inch of test specimen thickness. The specimen is then ready to be tested. Temperature shall be maintained within ±2°C (4°F) during the test.

[Note 2] Standard deviation on this estimate has been determined to be 15°C.

[Note 3] Data validation is covered in 8.8.2 and in Section 10.

8.5.2 To verify that the specimen is properly seated into the loading device and that the clip gage is properly seated, repeated preloading and unloading in the linear elastic range shall be applied. Load and unload the specimen between loads of 0.2 P_{max} and P_{max} (where P_{max} is the top precracking load) at least three times. Check the calculated crack size from each unloading slope against the average precrack size defined in 8.2.1. Refer to ASTM Standard Method E1152, Eq. (16) for C(T) specimens and to Eq. (19) for SE(B) specimens. Be aware that ice buildup at the loading clevis hole between tests can affect accuracy. Therefore, the loading pins and devices should be dried before each test. For working in fixtures, the elastic modulus to be used should be the nominally known value, E, for the material, and for side-grooved specimens, the effective thickness for compliance behavior is defined as:

$$B_e = 2B_N - B_N^2/B \ . \qquad (3)$$

For J calculations in Sect. 9, only B_N is used. All calculated crack sizes should be within 10% of the visual average and replicate determinations within 1% of each other. If the repeatability of determination is outside this limit, the test setup is suspect and should be thoroughly rechecked. After working-in the test fixtures, the load shall be returned to the lowest practical value at which the fixture alignment will not be lost.

8.6 Testing for K_{Jc} - All tests are conducted using displacement control; either by stroke or by clip gage devices. Load versus load-point displacement measurements shall be recorded. Periodic partial unloading can be introduced to determine the extent of slow-stable crack growth if it occurs. Alternative methods of measuring crack extension, for example the potential drop method, can be used.[13] If displacement measurements are made at a location other than at the load point, the ability to infer load point displacement within 2% of the absolute values is to be demonstrated. Also, to predict crack size from partial unloading slopes at a different location will require different compliance calibration equations than those recommended in 8.5.2. Table 2 in E561 contains equations that define compliance for other locations on the compact specimen.

8.6.1 Load specimens at a rate such that the time taken to reach load P_M lies between 0.1 and 10 min. P_M is nominally 40% of limit load; see

Standard E1152, 7.6.1, Eqs. (1) and (2). The crosshead speed during periodic partial unloadings may be as slow as needed to accurately estimate crack growth, but shall not be faster than the rate specified for loading.

8.6.2 Partial unloadings that are initiated between load levels P_M and $1.5P_M$ can be used to establish an "effective" value of E, E_e, such that the modulus normalized elastic compliance predicts an initial crack size within 0.001W of the actual initial crack size. This E_e should not differ from an expected or theoretical E of the material by more than 10% (see also E 561, Sect. 10). A minimum of two such unloadings shall be made and the slopes shall be repeatable within 1% of the mean value. Slow-stable crack growth usually develops at loads well above $1.5P_M$ and the spacing of partial unloadings is a matter of applying judgement. As an aim, every $0.01a_o$ increment of crack growth is suitable. Use E_e in place of E and B_e for thickness to calculate crack growth.

8.7 Test termination - After completion of the test, visually determine initial crack size and the extent of slow-stable crack growth and/or crack extension due to crack pop-in when applicable.

8.7.1 If the failure event is full cleavage fracture, measure the initial crack size using the nine-point method. Make the measurement at nine equally spaced points centered about the specimen centerline and extending to 0.01B from the free surfaces of plane sided specimens or near the side groove roots on side grooved specimens. Average the two near-surface measurements and combine the average of these two readings with the remaining seven crack measurements. Determine the average of those eight values. Measure slow-stable crack growth if it develops applying the same procedure. The measuring instruments shall have an accuracy of 0.001 in. (0.025 mm).

8.8 Qualification of Data

8.8.1 If any of the nine physical measurements of the starting crack size differ by more than 7% from the average defined in 8.7.1, the test is not valid.

8.8.2 Data sets (replicate tests at one temperature) generated at a test temperature at which several specimens approach the maximum toughness limitation of 7.5.1 and 10.2.2 may contain a specimen or

two that exceeds that toughness limitation and others that will not terminate in cleavage instability. For such tests that do not terminate in K_{Jc} fracture, the final K_J at test termination is not a valid K_{Jc} datum. For tests that terminate in cleavage but that have prior crack growth greater than 5% of the initial remaining ligament, $0.05(W - a_o)$, the K_{Jc} values are not valid. However, such data can be used in a data censoring procedure. Any test terminated with no cleavage fracture and where the final K_{Jc} is less than any of the valid cleavage K_{Jc} values in that data set is a nontest, the results of which cannot be used.

Data sets that contain all valid K_{Jc} values can be used without modification in Section 10. Data sets with invalid data but that have six or more valid data can be used with data censoring (10.1.2). Problems with excessive invalid data can be remedied by (1) testing at a lower test temperature, (2) testing with larger specimens, or (3) testing more specimens to satisfy data censoring requirements.

8.8.3 A discontinuity in a load-displacement record, where a distinct sound like a click may at times be detected emanating from the test system, is probably a pop-in event. All pop-in crack initiation K values for cracks that advance by a cleavage-driven mechanism are to be regarded as eligible K_{Jc} data. It is recognized that test equipment can at times introduce false pop-in indications in test records. If a questionable discontinuity develops, stop the loading as soon as possible and assess the compliance ratio by 9.2. If the compliance change calculated by 9.2 is greater than 2.1%, corresponding to more than a 1% increase in crack size, the recommended practice is to terminate the test, followed by heat tinting and breaking the specimen open at liquid nitrogen temperature. Measure the initial crack size and calculate K_{Jc} based on that crack size. Measure the post pop-in crack size visually and record it. If there is no visual evidence of cleavage type crack extension, then the K_{Jc} value at the discontinuity point is not a part of the K_{Jc} data distribution.

8.9 The fracture toughness evaluation of local brittle zones that are located in heat-affected zones of multipass weldments is not amenable to the statistical methods employed in the present practice.

9. CALCULATIONS

9.1 J-integral is determined at onset of cleavage fracture:

$$J_c = J_e + J_p . \quad (4)$$

9.1.1 Elastic component of J, (J_e), for compact specimens, C(T), is calculated as follows:

$$J_e = (K_e)^2/E ,$$

$$\text{where } K_e = [P/(BB_N W)^{1/2}]\, f\,(a_o/W) , \quad (5)$$

$$f(a_o/W)=\frac{(2+a_o/W)}{(1-a_o/W)^{3/2}}[0.886+4.64(a_o/W)-13.32(a_o/W)^2+14.72(a_o/W)^3-5.6(a_o/W)^4],$$

and a_o = initial crack size .

9.1.2 Elastic component of J,(J_e), for disk-shaped compact specimens, DC(T), is calculated as follows:

$$J_e = (K_e)^2/E ,$$

$$\text{where } K_e = [P/(BB_N W)^{1/2}]\, f(a_o/W) . \quad (6)$$

$$f(a_o/W)=\frac{(2+a_o/W)}{(1-a_o/W)^{3/2}}[0.76+4.8a_o/W)-11.58(a_o/W)^2+11.43(a_o/W)^3-4.08(a_o/W)^4],$$

and a_o = initial crack size .

9.1.3 Elastic component of J,(J_e), for SE(B) specimens of both B × B and B × 2B cross sections is calculated as follows:

$$J_e = (K_e)^2/E ,$$

$$\text{where } K_e = \{PS/[(BB_N)^{1/2} W^{3/2}]\} f(a_o/W) , \qquad (7)$$

$$f(a_o/W) = \frac{3(a_o/W)^{1/2}}{2[1+2(a_o/W)]} \quad \frac{1.99 - a_{o/W}(1-a_o/W)[2.15 - 3.93(a_o/W) + 2.7(a_o/W)^2]}{(1-a_o/W)^{3/2}},$$

and a_o = initial crack size.

9.1.4 The plastic component of J,(J_p), when slow-stable crack growth does not exceed 0.05 ($W - a_o$) is calculated as

$$J_p = \frac{\eta A_p}{B_N b_o}, \qquad (8)$$

where

A_p = $A - 1/2C_oP^2$,

A = $A_e + A_p$ (see Fig. 5) ,

C_o = the reciprocal of the initial elastic slope, V/P (Fig. 5),

b_o = initial remaining ligament.

For standard and disk compact specimens, $\eta = 2 + 0.522\, b_o/W$, and for bend bar specimens of both B × B and B × 2B cross sections, $\eta = 2$.

9.1.5 K_{Jc} is determined for each datum from J_c at onset of cleavage fracture. Assume plane stress for elastic modulus, E:

$$K_{Jc} = \sqrt{J_c E}. \quad (9)$$

9.1.6 The toughness level at which there is significant constraint loss for all specimen designs is given by the following:

$$K_{Jc\,(limit)} = (E b_o \sigma_{ys}/30)^{1/2}. \quad (10)$$

When a datum has exceeded the limit of Eq. (10), it is considered invalid for use in the statistical distribution.

9.2 Pop-in evaluation - Test records that can be used for K_{Jc} analyses are those that show complete specimen separation due to cleavage fracture and those that show pop-in. If an x-y record shows a small but perceptible discontinuity without the audible click of the typical pop-in, a mid-test decision will be needed. Following Fig. 6, determine the compliance ratio, C_i/C_o, and compare this to the value of the right-hand side of the following equation:

$$\frac{C_i}{C_o} > \left[1 + 0.01\,\eta\left(\frac{W}{a_o} - 1\right)\right], \quad (11)$$

where a_o is the nominal initial crack size (high accuracy on dimension a_o is not required here), and η is the parameter defined in 9.1.3. If C_i/C_o is greater than the calculated value, then refer to 8.8.3 under procedure.

9.3 Outlier - Occasionally a K_{Jc} value will appear to be well below the general population of K_{Jc} data. It is useful to examine such a value to determine if it belongs to the same population as the other data. At least 12 replicate K_{Jc} values are needed. Determine $K_{Jc(med)}$ including the outlier; then determine the 2% lower-bound confidence limit value of K_{Jc} as follows:

$$(K_{Jc})_{02} = 0.413\ K_{Jc(med)} + 11.74 \quad MPa\sqrt{m}. \quad (12)$$

An individual value of 12 or more that is less than $(K_{Jc})_{02}$ is likely to be an outlier.[Note 4] The median K_{Jc} derived from the remaining data can be used to characterize reference temperature, T_o.

10. PREDICTION OF SIZE EFFECTS AND TRANSITION TEMPERATURE

10.1 Weibull Fitting of Data Sets

10.1.1 Test replication - A data set consists of at least six replicate tests determined at one test temperature.

10.1.2 Data censoring - Weibull fitting can be performed on data sets that contain invalid K_{Jc} values (8.8.2) by means of data censoring.[2] However, all the data in the set must be obtained from one specimen size and have at least six valid K_{Jc} values to proceed. The procedure is to rank all data in order of increasing value as illustrated in the example case worked in Annex A, Sect. IV. The invalid data are expected to be those that exceed the limit given in para. 10.2.2 and data of the highest fracture toughness rank can be censored. Invalid data are then assigned a K_{Jc} value that corresponds to the validity limit.

10.1.3 Fitting data by three-parameter Weibull - The three-parameter Weibull model fitting of data cumulative probability distributions is illustrated with simple example cases worked in Annex A. At least six valid K_{Jc} data are required. Data are fitted using a fixed Weibull slope of 4 and fixed K_{min} of 20 MPa√m. Only the appropriate scale factor, K_o, needs to be determined. On occasion, the plotted data will not follow the theoretical Weibull slope of 4. It should be understood that there is a finite probability that this will happen, especially with small data sets, but this is not a consistent pattern of behavior. Selection of an alternate Weibull slope or alternate K_{min} value to fit such data is not recommended in this practice. Also, it is important to understand that K_{min} does not necessarily represent an experimentally achievable minimum fracture toughness value, but instead is a mathematical data-fitting parameter.

10.2 Prediction of Specimen Size Effects on $K_{Jc(med)}$ or Single K_{Jc} Datum

---

[Note 4] Data rejection is a risky practice since outliers potentially could be the result of a serious material inhomogeneity problem.

10.2.1 Limitations - Weakest-link theory provides the basis for specimen size adjustments. Size effects can be defined only within a specific part of the transition temperature range.

10.2.2 Limit on constraint loss - At high fracture toughness, loss of constraint becomes the concern since weakest-link theory assumes that all specimens have controlled and similar conditions of constraint. The upper bound is set on the basis of K_{Jc}, specimen size, and material yield strength. See Eqs. (1) and (10). At mid-transition range, a lower-bound limit of toughness loss corresponding to increased specimen size toward infinity is a commonly assumed postulate. Methods for estimating this limit from small specimen data are the subject of current research and cannot be specified at the present time.

10.2.3 Lower-shelf toughness limit - As the lower-shelf toughness at low temperatures is approached, specimen size effects diminish due to a change in the cleavage crack triggering mechanism.[14] This limit develops when plastic deformation at the crack tip is highly localized. Size effects tend to vanish at test temperatures of about 90°C (160°F) below reference temperature, T_o (defined in 10.3.1). This limitation indicates a toughness level below which Eqs. (13) and (15) should not be used. Also, the lower shelf data cannot be expected to deliver an accurate estimate of reference temperature, T_o, defined in 10.3.

10.2.4 Predicting size effects - To predict the Weibull K_o, $K_{Jc(med)}$, or K_{Jc} for specimens of another thickness, B_x, use Eq. (13). As an example for adjustment of median K_{Jc}:

$$K_{(med)x} = 20 + [K_{Jc(med)} - 20]\left(\frac{B_o}{B_x}\right)^{1/4}, \qquad M \tag{13}$$

where

$K_{Jc(med)}$ = median K_{Jc} for test data,
B_o = thickness of test specimens,
B_x = thickness of prediction.

10.3 Transition Temperature Curve (Master Curve)

10.3.1 Master curve - Transition temperature K_{Jc} data tend to conform to a common toughness versus temperature curve shape in the same manner as the ASME K_{Ic} and K_{IR} lower-bound design curves.[15] For this practice, the shape of the median K_{Jc} toughness, $K_{Jc(med)}$, for 1T specimens is described by:

$$K_{Jc(med)} = 30 + 70\exp[0.019(T - T_o)], \text{ MP} \quad (14)$$

10.3.2 Effects of specimen thickness on K_{Jc} - Data equivalent to that for a 1T specimen size can be calculated from data measured with specimens of a different size by using the following equation:

$$K_{Jc(1T)} = 20 + [K_{Jc(x)} - 20]\left(\frac{B_x}{B_{1T}}\right)^{1/4}, \text{ MPa}\sqrt{} \quad (15)$$

where B_x is the test specimen thickness.

10.3.3 Positioning of the master curve - For optimum placement of the master curve, Eq. (14), 1T size specimens should be tested at a temperature near to T_o. T_o is the temperature at which 1T specimens have median K_{Jc} = 100 MPa√m. Charpy V-notch (CVN) data, preferably TL orientation, can be used as an aid for predicting a suitable test temperature (see 8.4).

10.3.4 Reference temperature (T_o) determination - When tests are made at one selected test temperature, at least six valid K_{Jc} values are needed. The uncertainty in reference temperature, T_o, determined therefrom is covered by margin adjustment (see Annex C). Uncertainty in T_o can be reduced by testing more groups of specimens at other temperatures. However, testing at temperatures near the lower shelf of the transition range should not be expected to produce an accurate estimate of T_o. Excessive censoring of data at high test temperatures is also not likely to produce good T_o estimates. Median K_{Jc} of the data set can be calculated from K_o, Eq. (A3), or otherwise it can be determined by setting P_f = 0.5 in Eq. (A1), obtaining y = –0.3665. Then use the

Weibull plot in a similar way as the K_o example in Fig. A1. Determine T_o from $K_{Jc(med)}$ using the following:

$$T_o = T - (0.019)^{-1} \ln\left[\frac{K_{Jc(med)} - 30}{70}\right], °C \qquad (16)$$

where $K_{Jc(med)}$ is the median value of K_{Jc} for 1T specimens tested at temperature T. See 10.3.2 for size effect conversions and Annex B for an example determination. Temperature T_o should be relatively independent of the test temperature chosen. Determine an average T_o value. Highly unequal T_o values from several test temperatures indicate that the data are not fitting the master curve. If T_o values obtained from two or more test temperatures differ by more than 20°C, then the correctness of Eq. (14) for defining the transition temperature curve for the test material is subject to question.

10.3.5 Uses for master curve - The master curve can be used to define a transition temperature shift due to metallurgical damage mechanisms. Fixed values of Weibull slope and median K_{Jc} define the standard deviation and therefore the degree of data scatter. This information can be used to calculate confidence limits on toughness, for the specimen reference size chosen, by means of a margin adjustment to T_o, to offset the uncertainty in reference temperature due to small sample sizes (see Annex C). The data scatter characteristics modeled here can be of use in probabilistic fracture mechanics analysis.

11. REPORT

11.1 The report shall contain the following information:

11.1.1 Specimen type, specimen thickness, B, net thickness, B_N, specimen width, W.

11.1.2 Specimen initial crack size.

11.1.3 Visually measured slow-stable crack growth to failure.

11.1.4 Crack plane orientation according to Standard E616.

11.1.5 Test temperature.

11.1.6 Number of valid specimens and total number of specimens tested at each temperature.

11.1.7 Crack pop-in and compliance ratio, C_i/C_o.

11.1.8 Material yield strength and tensile strength.

11.1.9 Median K_{Jc} (MPA$\sqrt{m}$).

11.1.10 Reference temperature on master curve, T_o (°C).

11.2 The report may contain the following supplementary information:

11.2.1 Specimen identification codes.

11.2.2 Fatigue precracking condition in terms of K_{max} for the last 0.64 mm (0.025 in.) of precrack growth.

11.2.3 Difference between maximum and minimum crack length measurement expressed as a percentage of the initial crack size.

11.2.4 Measured pop-in crack extensions.

11.2.5 Load-displacement record.

12. PRECISION AND BIAS

12.1 Precision - The variability of measurement of K_{Jc} data is an integral part of this test procedure. It has been determined that most K_{Jc} data distributions for tests made at one test temperature with specimens that satisfy the geometry requirements of this procedure, that the Weibull slope for the population will be 4. The above claim applies to the three-parameter Weibull in which K_{min} of 20 MPa$\sqrt{m}$ is a deterministic parameter of the statistical model. Small numbers of replicate K_{Jc} determinations, including the mandatory number of six specimens, at times may not appear to accurately represent the population distribution and apparently poor fits to a Weibull slope of 4 should not be cause for concern. The median K_{Jc} will be accurate to within 20% and it is this value that is used to establish the reference temperature, T_o, which in turn is used to position the 1TCT master curve on the temperature axis. If reference temperatures are calculated from median K_{Jc} values at several test temperatures, then all values of T_o should be within a scatter band of 20°C, otherwise the master curve should not be used to characterize the K_{Jc} fracture toughness of a material.

12.2 Bias - There is no accepted "standard" value for the fracture toughness of an arbitrarily chosen material. In the absence of the true "known" value, any statement concerning bias is not meaningful.

13. REFERENCES

1. Anderson, T. L., Steinstra, D., and Dodds, R. H., "A Theoretical Framework for Addressing Fracture in the Ductile-Brittle Transition Region," *Fracture Mechanics, 24th Volume, ASTM STP 1207*, American Society for Testing and Materials, Philadelphia, 1994, pp. 185-214.

2. Steinstra, D. I. A., "Stochastic Micromechanical Modeling of Cleavage Fracture in the Ductile-Brittle Transition Region," MM6013-90-11, Ph.D. thesis, Texas A & M University, College Station, Texas, August 1990.

3. Landes, J. D., and McCabe, D. E., "Effect of Section Size on Transition Temperature Behavior of Structural Steels," *Fracture Mechanics: Fifteenth Symposium, ASTM STP 833*, University of Maryland, 1984, pp. 378-392.

4. Wallin, K., "Recommendations for the Application of Fracture Toughness Data for Structural Integrity Assessments," *Proceedings of the Joint IAEA/CSNI Specialists Meeting on Fracture Mechanics Verification by Large-Scale Testing*, NUREG/CP-0131 (ORNL/TM-12413), October 1993.

5. Paris, P. C., "Fracture Mechanics in the Elastic-Plastic Regime," *Flaw Growth in Fracture, ASTM STP 631*, American Society for Testing and Materials, Philadelphia, August 1976.

6. McCabe, D. E., *Evaluation of Crack Pop-ins and the Determination of their Relevance to Design Considerations*, NUREG/CR-5952 (ORNL/TM-12247), February 1993.

7. Turner, C. E., "The Eta Factor," *Post Yield Fracture Mechanics*, Second Ed., Elsevier Applied Science Publishers, London and New York, 1984, pp. 451-459.

8. Wallin, K., "The Scatter in K_{Ic} Results," *Engineering Fracture Mechanics*, 19(6) 1085-1093 (1984).

9. Nevalainen, M., and Dodds, R. H., *Numerical Investigation of 3D Constant Effects on Brittle Fracture of SE(B) and C(T) Specimens*, UIUL ENG-95-2001, University of Illinois, Champaign-Urbana, 1995.

10. Underwood, J. H., Troiano, E. J., and Abbott, R. T., "Simpler J_{Ic} Test and Data Analysis Procedures for High Strength Steels," pp. 410-21 in *Fracture Mechanics: Twenty-Fourth Volume, ASTM STP 1207*, American Society for Testing and Materials, Philadelphia, 1994.

11. Landes, J. D., "J Calculation from Front Face Displacement Measurements of a Compact Specimen," *International Journal of Fracture*, 16 (1980).

12. Wallin, K., "A Simple Theoretical Charpy V-K_{Ic} Correlation for Irradiation Embrittlement," *ASME Pressure Vessels and Piping Conference, Innovative Approaches to Irradiation Damage and Fracture Analysis*, PVP-Vol. 170, American Society of Mechanical Engineers, July 1989.

13. Schwalbe, K. H., Hellmann, D., Heerens, J., Knaack, J., and Mueller-Roos, J., "Measurement of Stable Crack Growth Including Detection of Initiation of Growth Using Potential Drop and Partial Unloading Methods," *Elastic-Plastic Fracture Test Methods, Users Experience, ASTM STP 856*, American Society for Testing and Materials, Louisville, April 1983.

14. Heerens, J., Read, D. T., Cornec, A., and Schwalbe, K.-H., "Interpretation of Fracture Toughness in the Ductile-to-Brittle Transition Region by Fractographical Observations, pp. 659-78 in *Defect Assessment in Components - Fundamentals and Applications*, J. G. Blauel and K.-H. Schwalbe, eds., ESIS/EGF9, Mechanical Engineering Publications, London, 1991.

15. *ASME Boiler and Pressure Vessel Code. An American National Standard*, Sect. XI, Article A-4000, "Rules for Inservice Inspection of Nuclear Power Plant Components," American Society of Mechanical Engineers, New York, 1993.

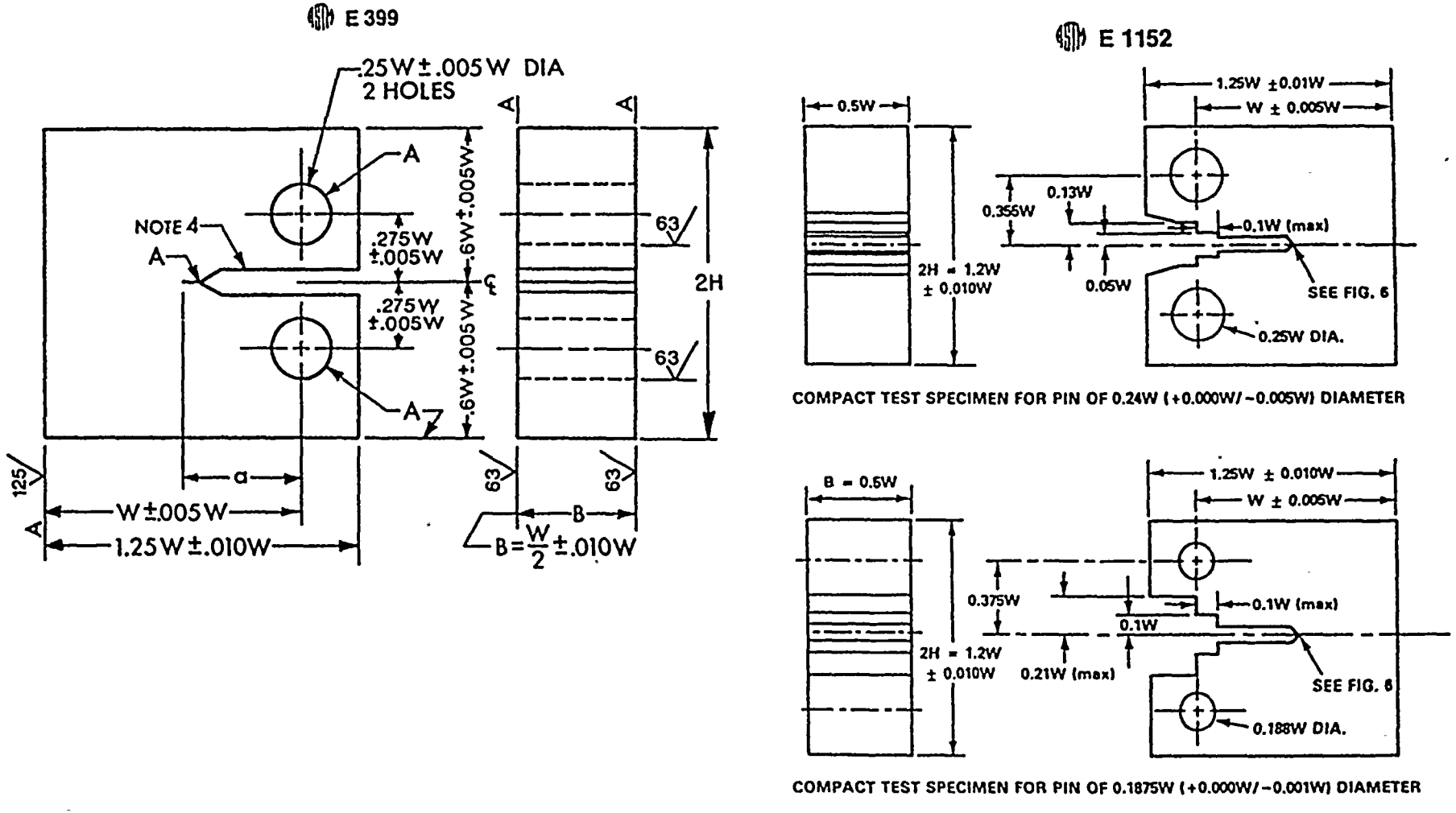

Fig. 1. Recommended compact specimen designs.

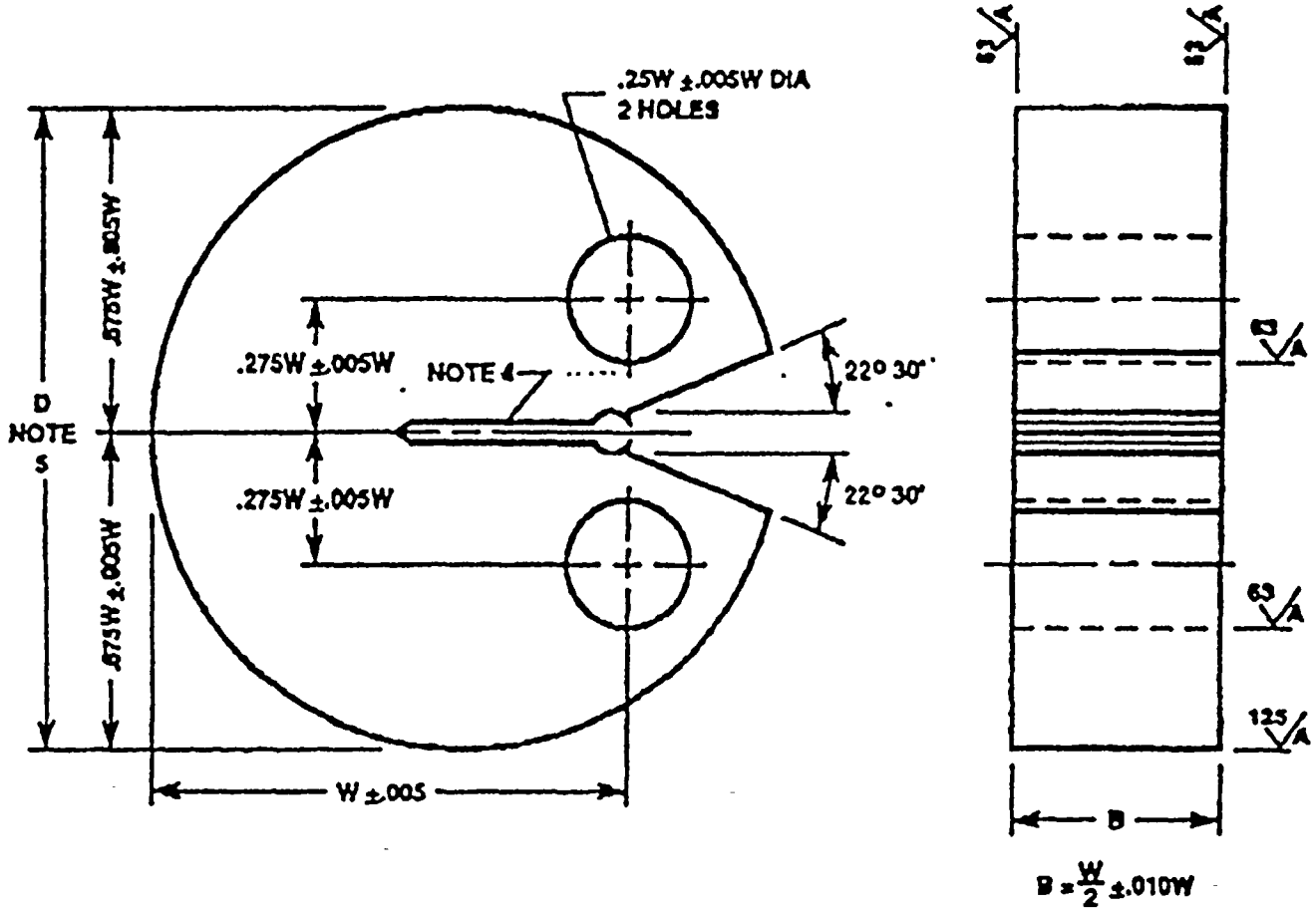

Fig. 2. Disk-shaped compact specimen DC(T) standard proportions. Integral or attached knife edges for clip gage attachment may be used.

ORNL-DWG 93-12707

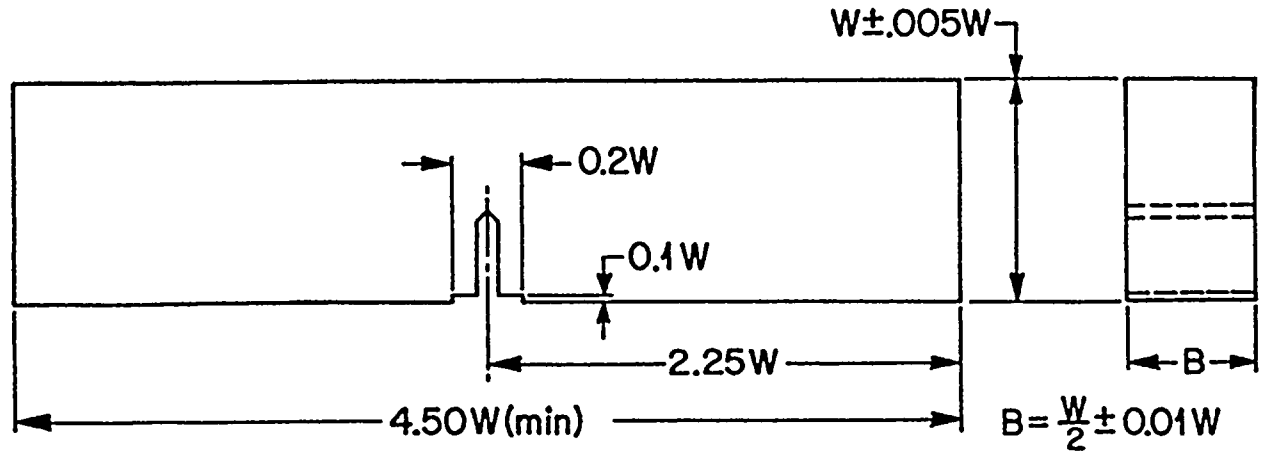

MACHINED NOTCH

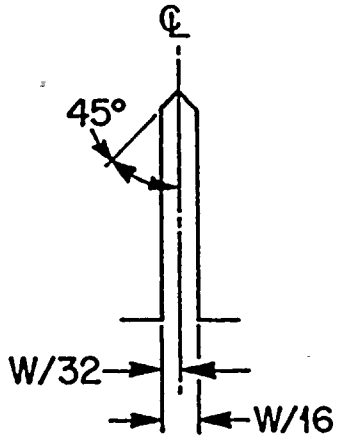

USE 90° INCLUDED ANGLE CUTTER WITH 0.003 in. TIP RADIUS. NOTCH TO BE 0.003 in. ± 0.002 in. RADIUS.

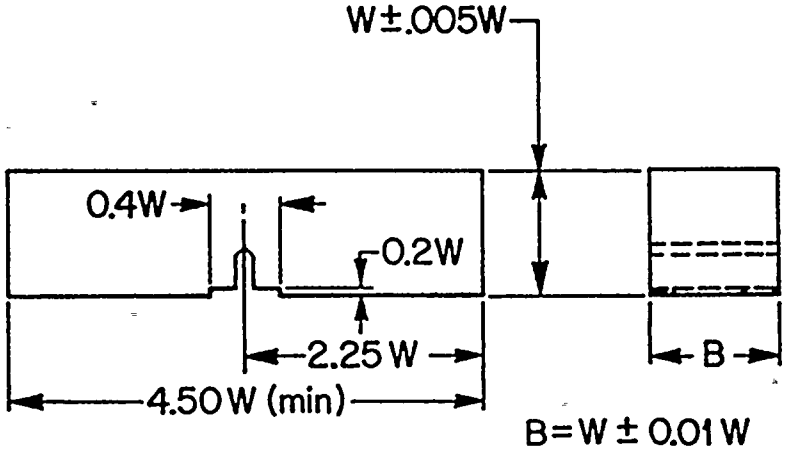

NOTE:

1) ALL SURFACES SHALL BE PERPENDICULAR AND PARALLEL WITHIN 0.001W TIR. SURFACE FINISH 64 v.
2) CRACK STARTER NOTCH SHALL BE PERPENDICULAR TO SPECIMEN SURFACES TO WITHIN ±2°.

Fig. 3. Recommended bend bar specimen design.

ORNL-DWG 93-6630

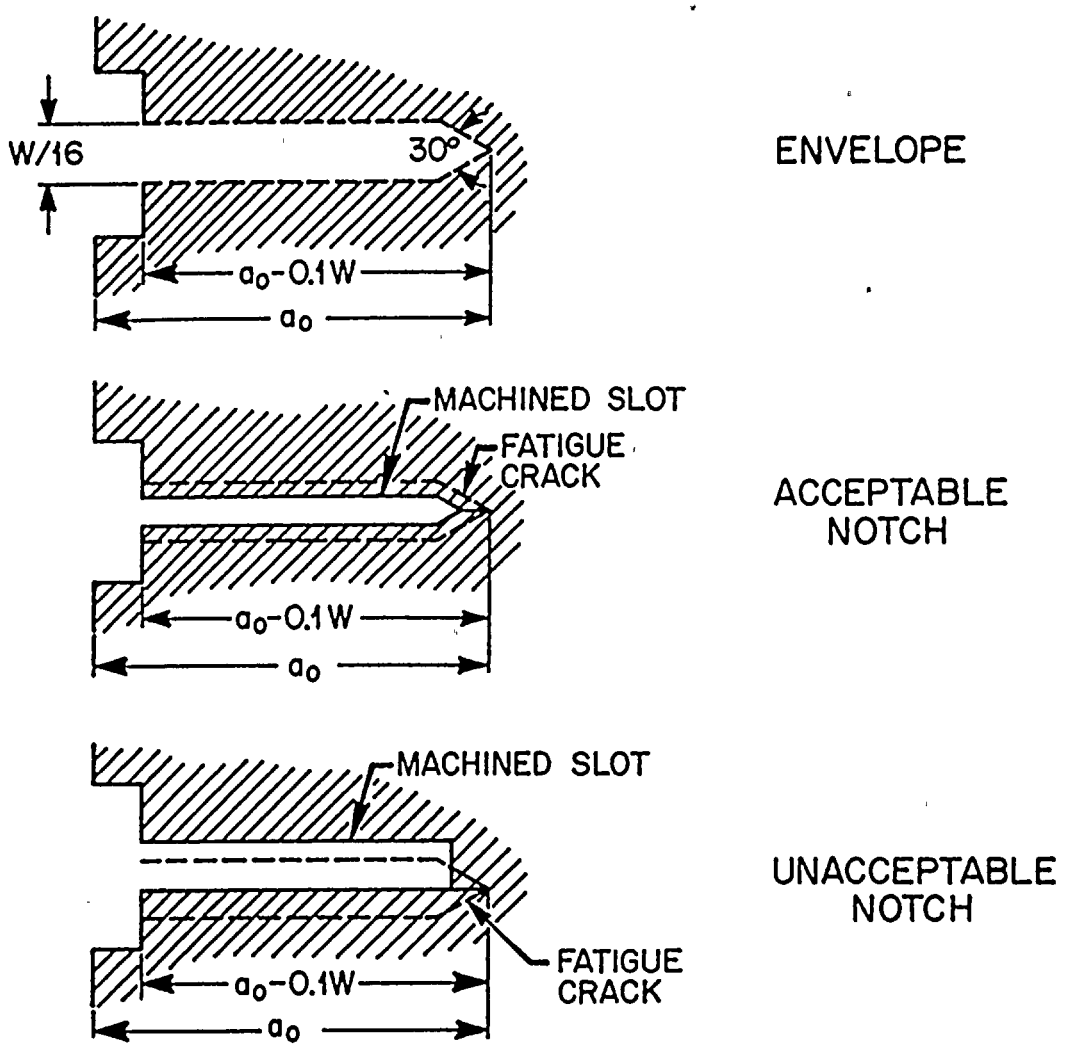

Fig. 4. Envelope crack starter notches.

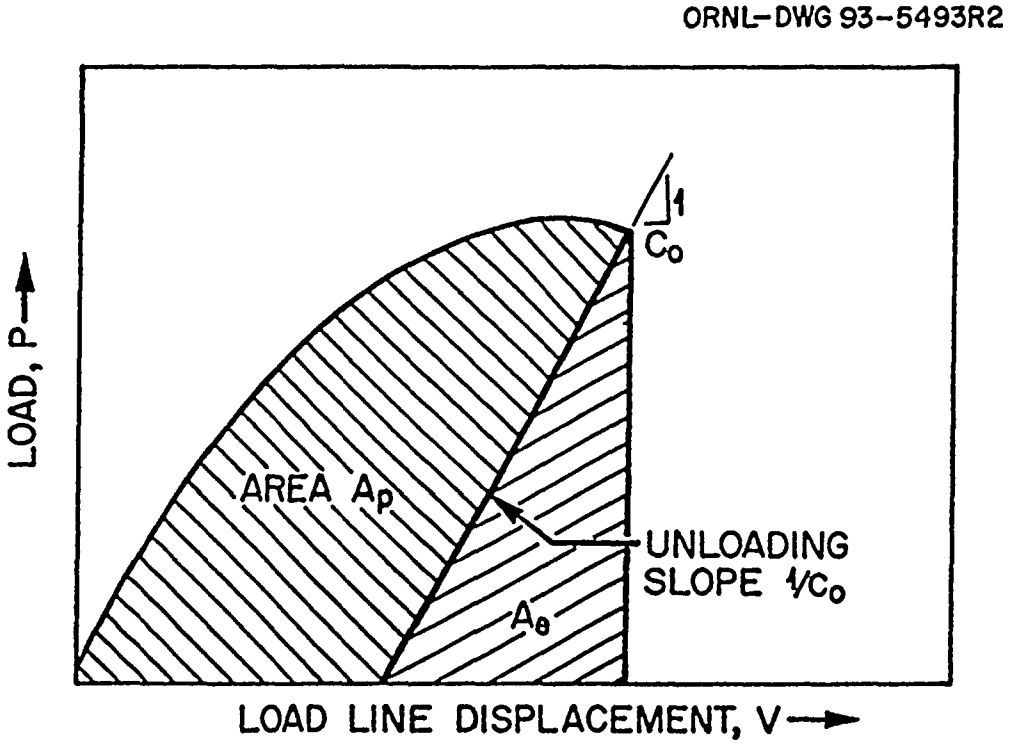

Fig. 5. Definition of the plastic area for J_p calculations.

ORNL-DWG 93-5495R

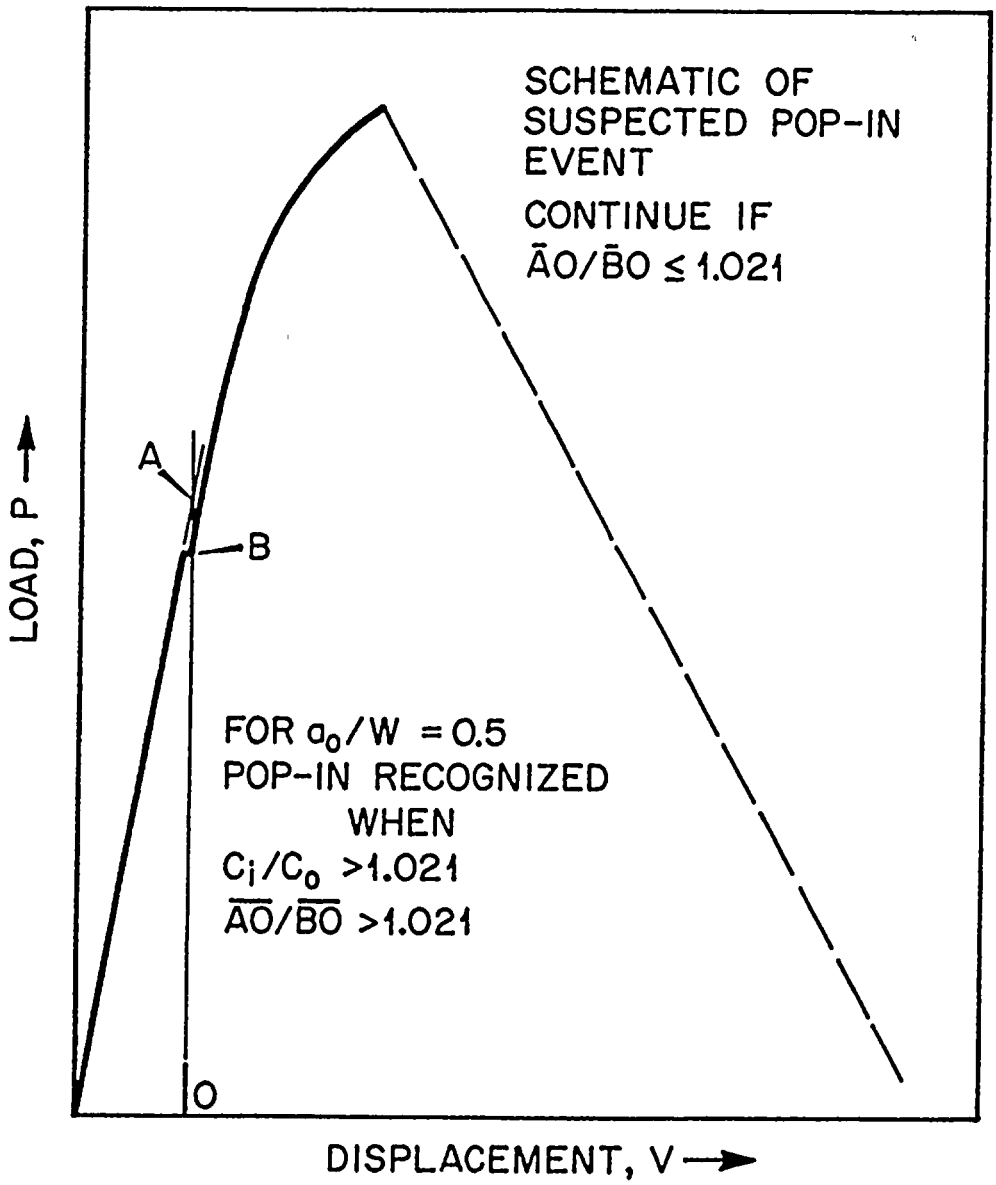

Fig. 6. Schematic of pop-in magnitude evaluation.

ANNEX A
WEIBULL FITTING OF DATA

I. DESCRIPTION OF THE WEIBULL MODEL

The three-parameter Weibull model is used to fit the relationship between K_{Jc} and the cumulative probability for failure, P_f. The term P_f is the probability for failure at K_{Jc} for an arbitrarily chosen specimen from the population of specimens. This can be calculated from the following:

$$P_f = 1 - \exp - \left[(K_{Jc} - K_{min})/(K_o - K_{min})\right]^b . \qquad (A1)$$

Ferritic steels of yield strengths ranging from 275 to 825 MPa (40 to 120 ksi) will have fracture toughness distributions of nearly the same shape when K_{min} is set at 20 MPa$\sqrt{m}$ (18.2 ksi$\sqrt{in.}$). This shape is defined by the Weibull exponent, b, which tends to be constant at 4. Scale parameter, K_o, is the data-fitting parameter and the procedure is described in Sect. II.

II. DETERMINATION OF SCALE PARAMETER, K_o, AND MEDIAN K_{Jc} USING THE MAXIMUM LIKELIHOOD METHOD

The following example demonstrates the procedure.

Table A1. Six 4T compact specimens of A 533 grade B (–75°C)

Rank (i)	K_{Jc} (MPa√m)
1	59.1
2	68.3
3	77.9
4	97.9
5	100.9
6	112.4

$$K_o = \left[\sum_{i=1}^{N} (K_{Jc(i)} - K_{min})^4/(N - 0.3068) \right]^{1/4} + K_{min}$$

$$K_{min} = 20 \text{ MPa } \sqrt{m} \qquad \text{(A2)}$$

$$N = 6$$

$$K_o = 94.1 \text{ MPa}\sqrt{m}$$

Median K_{Jc} is obtained as follows:

$$K_{Jc(med)} = (K_o - K_{min})[\ln(2)]^{1/4} + K_{min} \qquad \text{(A3)}$$

$$K_{Jc(med)} = 87.6 \text{ MPa}\sqrt{m}$$

III. DEVELOPMENT OF WEIBULL PLOTS

Data points of Table A1 are converted to Weibull coordinates using:

$$Y_i = \ln\left\{\ln[1/(1 - \hat{P}_{f(i)})]\right\}$$

$$\text{where } \hat{P}_{f(i)} = \frac{(i - 0.3)}{(N + 0.4)} \text{ (see Note A1)} \qquad \text{(A4)}$$

$$N = \text{number of tests}$$

$$X_i = \ln[K_{Jc(i)} - K_{min}] \qquad \text{(A5)}$$

$$\text{where } K_{min} = 20 \text{ MPa}\sqrt{m}$$

The regression line with a slope of 4 is fitted to the data points in the following way:

$$Y = 4X + Y_o$$

$$\text{where } Y_o = -4 \ln(K_o - K_{min}) \qquad \text{(A6)}$$

$$K_{min} = 20 \text{ MPa}\sqrt{m}$$

For Table A1 data, $Y_o = -17.08$. Therefore, $Y = 4X - 17.08$ (see Fig. A1).

[Note A1: The use of ^ over variables such as P_f denotes the value is fixed with no variance.]

IV. DATA CENSORING

K_{Jc} data can be invalid because of not satisfying the requirements of Paragraph 8.8. However, such data can be used in a censoring practice. All data must come from one specimen size. Only the highest ranked data can be censored. There must be six valid K_{Jc} values in the group. An example is given below for the following table of data:

Table A2. K_{Jc} data on 4T size bend bars of A 533 grade B steel tested at 10°C

Rank (i)	K_{Jc} (MPa√m)	Δa_p (mm)
1	365.5	1.2
2	403.1	1.4
3	409.6	1.8
4	470.2	2.3
5	549.8	4.5
6	572.0	4.9
7	632.3[a]	6.9
8	647.1[a]	10.3
9	741.3[a]	15.4

[a]Censored datum.

Determine scale parameter, K_o, using the following:

From $(EB\sigma_{ys}/30)^{1/2}$; K_{Jc} (limit) = 606 MPa√m.
Censor data ranked = 7, 8, 9.
(Substitute K_{Jc} = 606 MPa for these in Eq. (A7).
r = 6

$$K_o = \left[\sum_{I=1}^{N} (K_{Jc(I)} - K_{min})^4/(r - 0.3068)\right]^{1/4} + K_{min} \qquad (A7)$$

K_o = 595.7 MPa√m .

V. WEIBULL SLOPE FIT TO CENSORED DATA SET

$$Y_o = -4 \ln (K_o - K_{min})$$

$$K_{min} = 20 \text{ MPa}\sqrt{m}$$

for Table A2 data, $Y_o = -25.42$

Therefore: $Y = 4X - 25.42$ (see Fig. A2)

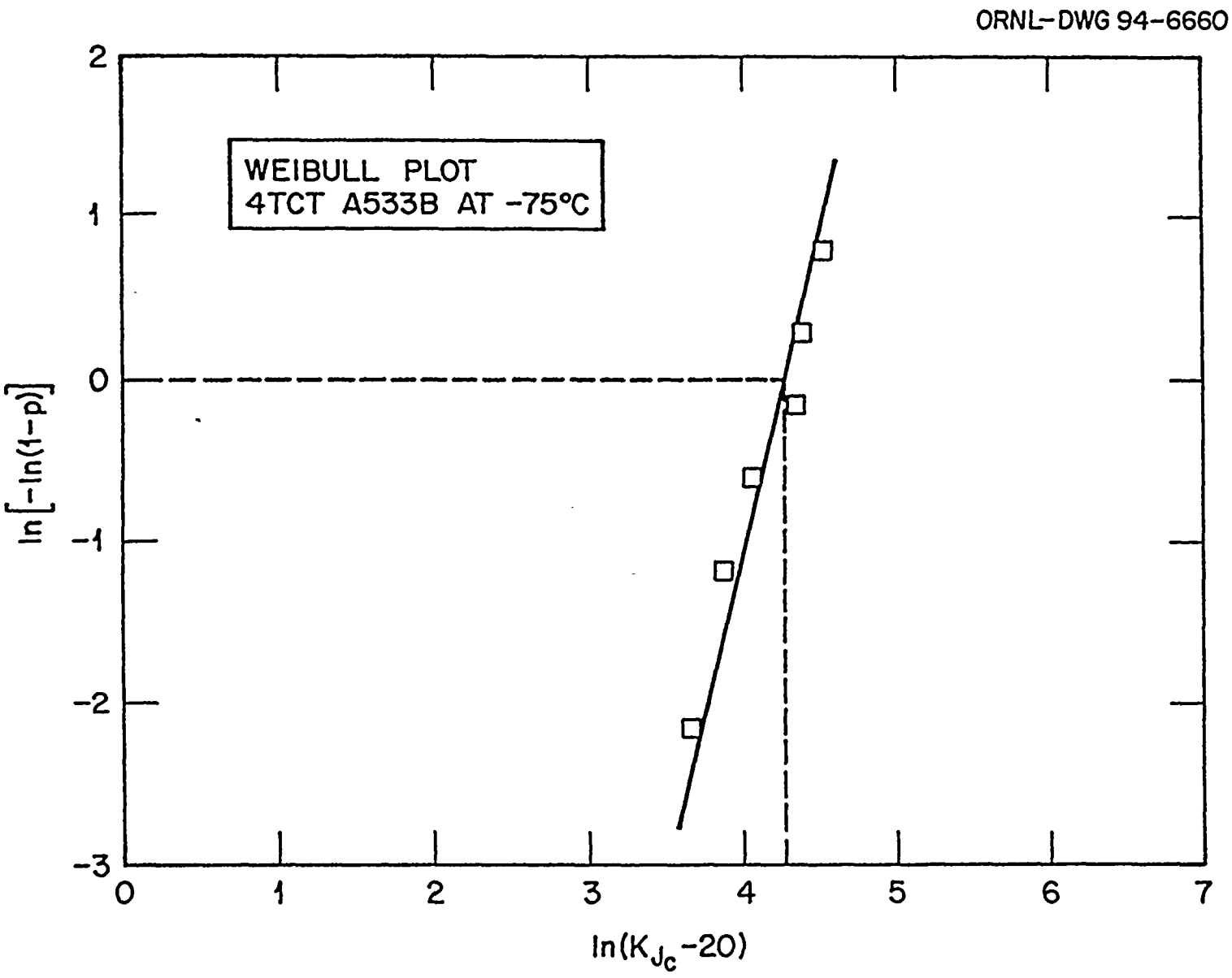

Fig. A1. Weibull plot showing identification of [K_o – 20] MPa√m point.

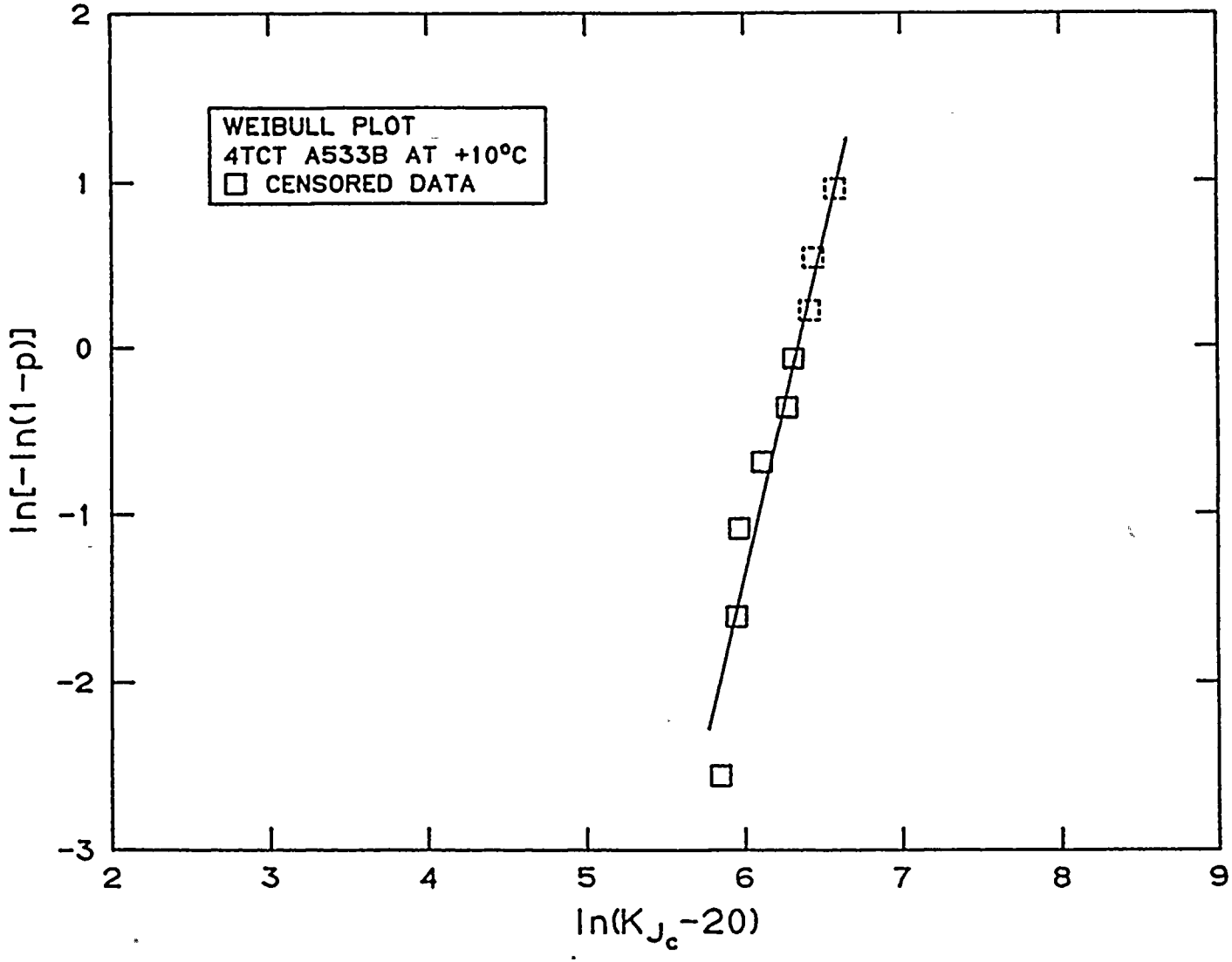

Fig. A2. Weibull plot with three censored data. The fitted line of Weibull slope = 4 comes from maximum likelihood derived K_o.

ANNEX B

MASTER CURVE FIT TO DATA

I. Select test temperature (8.4):

Six 1/2T compact specimens
A 533 grade B base metal
Test temperature, T = –75°C

II. Rank data and convert to K_{Jc}, equivalence for 1T compact size (10.3.2):

Rank (i)	K_{Jc} – 1/2T (MPa√m)	K_{Jc} – 1T (MPa√m)	P_f	$\ln[(K_{Jc}) - 20]$	$\ln[\ln(1/1 - P_f)]$
1	91.4	80.0	0.109	4.09	–2.155
2	103.1	89.9	0.266	4.21	–1.175
3	120.3	104.3	0.422	4.43	–0.602
4	133.5	115.4	0.578	4.56	–0.147
5	144.4	124.6	0.734	4.65	0.282
6	164.0	141.1	0.891	4.80	0.794

III. Plot and determine best fit to data with slope b = 4 and K_{min} = 20. See Fig. B1.

At $\ln\{\ln[1/(1 - P_f)]\} = 0$

$K_{Jc} = K_o$

$K_o = 118.5$ MPa√m

$K_{Jc(med)} = [\ln(2)]^{1/4} (K_o - 20) + 20 = 109.9$ MPa√m

IV. Position master curve:

$T_o = T - (0.019)^{-1} \ln [(K_{Jc(med)} - 30)/70]$

$= -75 - \ln[(109.9 - 30)/70]/0.019 = \underline{-82°C}$. (B1)

V. Master curve:

$$K_{Jc(med)} = 30 + 70 \exp[0.019(T + 82)] . \quad \text{(B2)}$$

See Fig. B2.

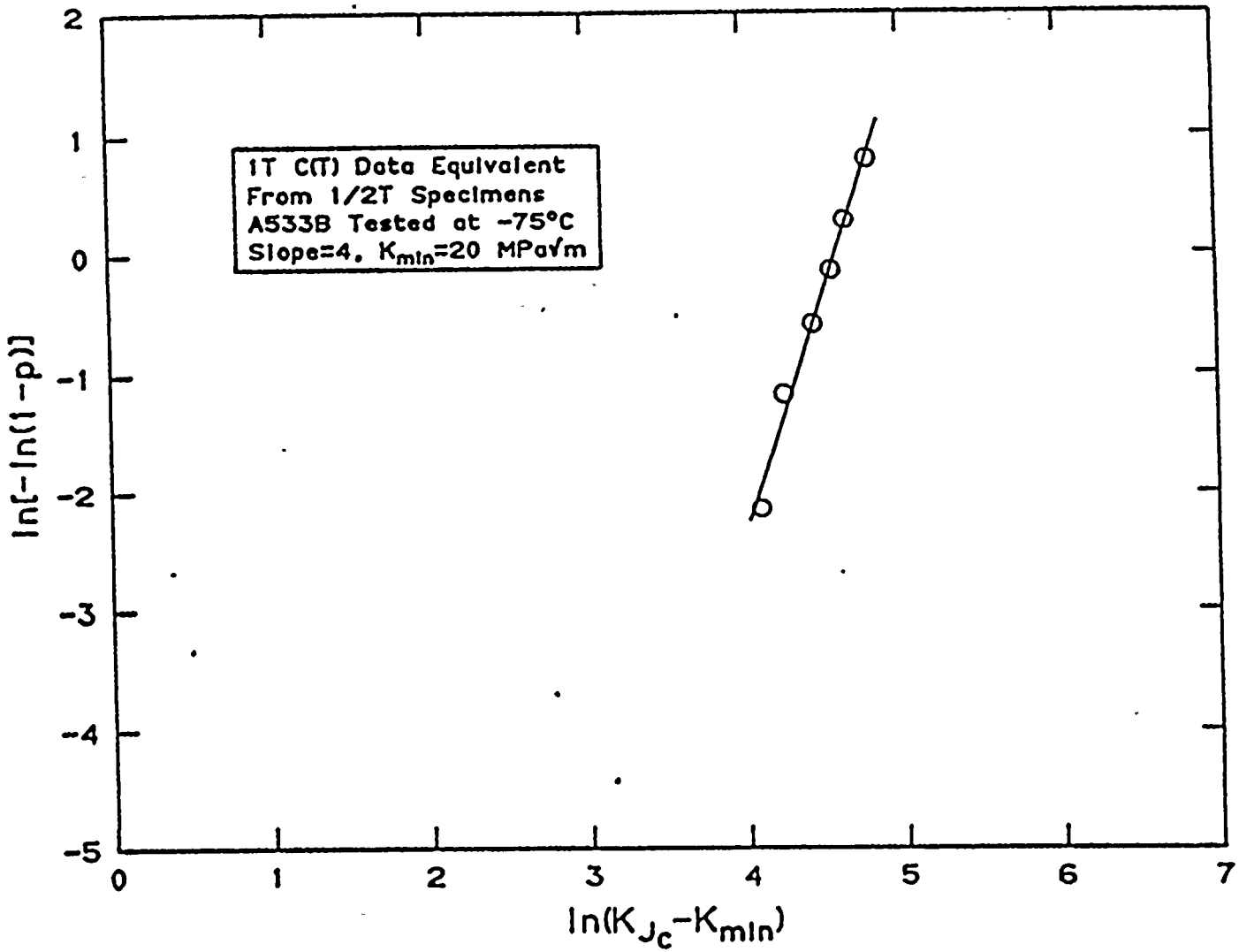

Fig. B1. Weibull plot of 1T equivalent K_{J_c} values.

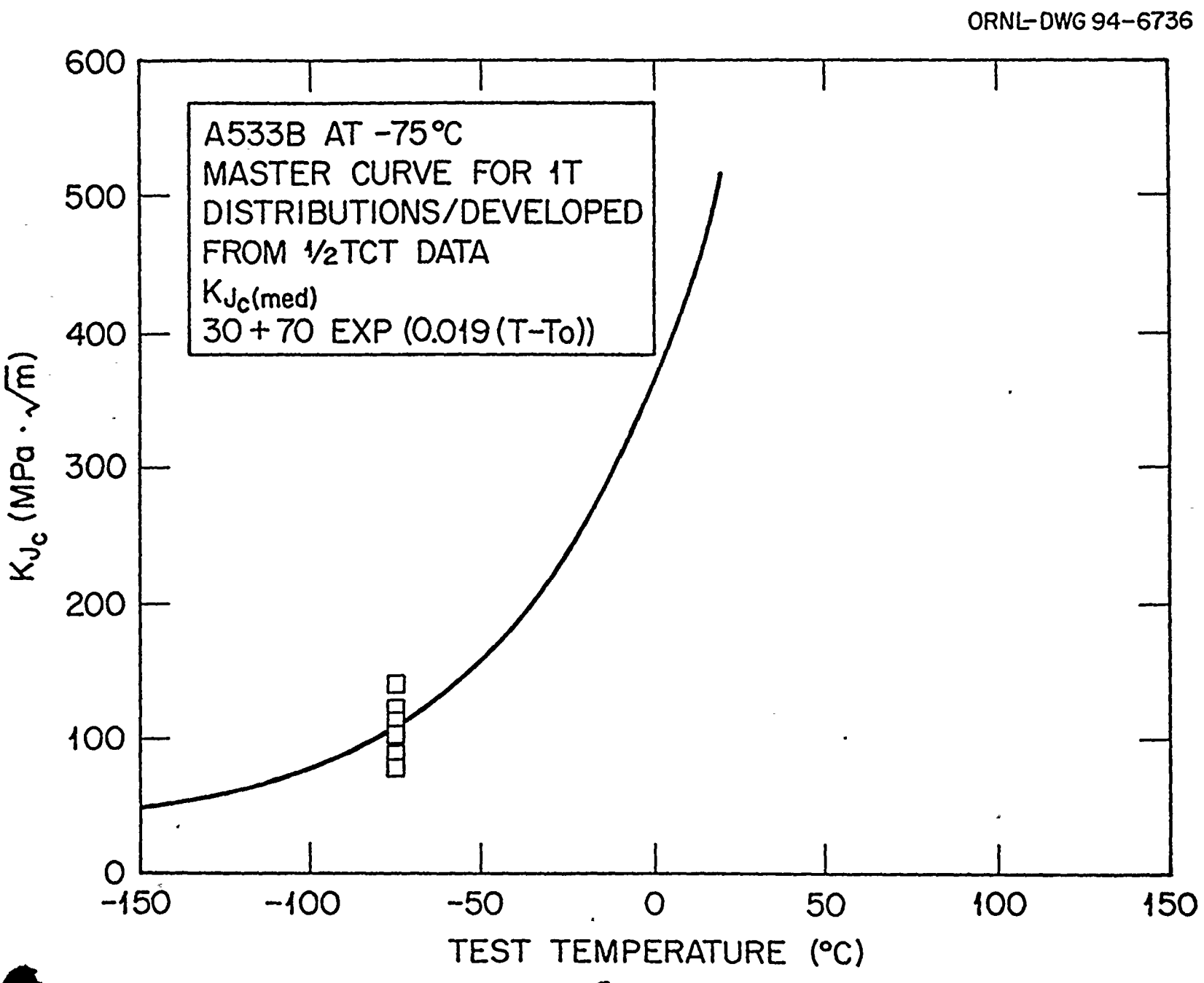

Fig. B2. Master curve based on 1/2T data tabulated in step II.

ANNEX C

CALCULATION OF CONFIDENCE LIMITS

Data scatter is a function of Weibull slope and K_{min}, so, given that these are constant values, standard deviation is automatically defined. Specifically, with slope of 4 and K_{min} = 20 MPa√m standard deviation is defined by the following:

$$\sigma = 0.28\, K_{Jc(med)}[1 - 20/K_{Jc(med)}]\,. \qquad \text{(C1)}$$

I. Confidence Limits - Lower-bound confidence (1, 2, 3, 4, 5, and 10%) and upper-bound confidence (90, 95, 96, 97, 98, and 99%) curves can be calculated using the following:

$$K_{CL} = D_1 + D_2 \exp\,[0.019(T - T_o)]\,, \qquad \text{(C2)}$$

where T is the temperature value on the abscissa in °C and T_o is the reference temperature of the master curve, °C. See Fig. C1 for 5 and 95% confidence limits. As an example, the 5% confidence bound from the Annex B example is

$$K_{(0.05)} = 25.4 + 38.7 \exp\,[0.019(T + 82)]\,. \qquad \text{(C3)}$$

Table C1.

Confidence bound (CL) (%)	Z_x[a]	Coefficients	
		D_1	D_2
01	2.320	23.5	24.5
02	2.055	24.3	30.0
03	1.88	24.7	33.2
04	1.75	25.1	35.7
05	1.645	25.4	37.8
10	1.280	26.4	44.9
90	1.280	33.6	95.1
95	1.645	34.6	102.2
96	1.75	34.9	104.3
97	1.88	35.3	106.8
98	2.055	35.8	110.3
99	2.320	36.5	115.5

[a] Z_x is the standard normal deviate taken as the difference between a specific value of fracture toughness and the median toughness for the population expressed as a multiple of the standard of deviation, see Eq. (C1). The tabulated values are for normal or gaussian distributions. These values are within 3% of more rigorously determined values for Weibull distributions where b = 4 and K_{min} = 20 MPa√m. x represents a specified probability.

II. The margin-adjusted confidence curve is a special confidence limit case for which a margin is added to cover the uncertainty associated with the use of only a few specimens to make a single estimate of temperature, T_o. Standard deviation for estimates of T_o is inversely related to $K_{Jc(med)}$, but near the 100-MPa√m toughness level it becomes nearly constant and is approximated by the following:

$$\sigma = 18°C / \sqrt{N}. \qquad (C4)$$

N is the total number of specimens that were used to establish the temperature T_o. In this case, the two tail normal deviate, Z_x, based on the estimate of a mean should be used. Specifically, the selection of the confidence limit, $\propto$, on T_o is a matter for engineering decision, but an example case for 85% confidence on T_o of the data shown in Annex B is illustrated as follows:

$$\Delta T_o = \sigma(1Z_{85}) = \frac{18}{\sqrt{6}}\,(1 \times 1.44) = 10\,.$$

$$T_o(\text{margin}) = T_o + \Delta T_o = -82 + 10 = -72.$$

Then the margin adjusted 5% confidence limit is:

$$K_{Jc(0.05)} = 25.4 + 37.8 \exp\left[0.019(T + 72)\right]. \qquad \text{(C5)}$$

See Fig. C2, dashed line (LB).

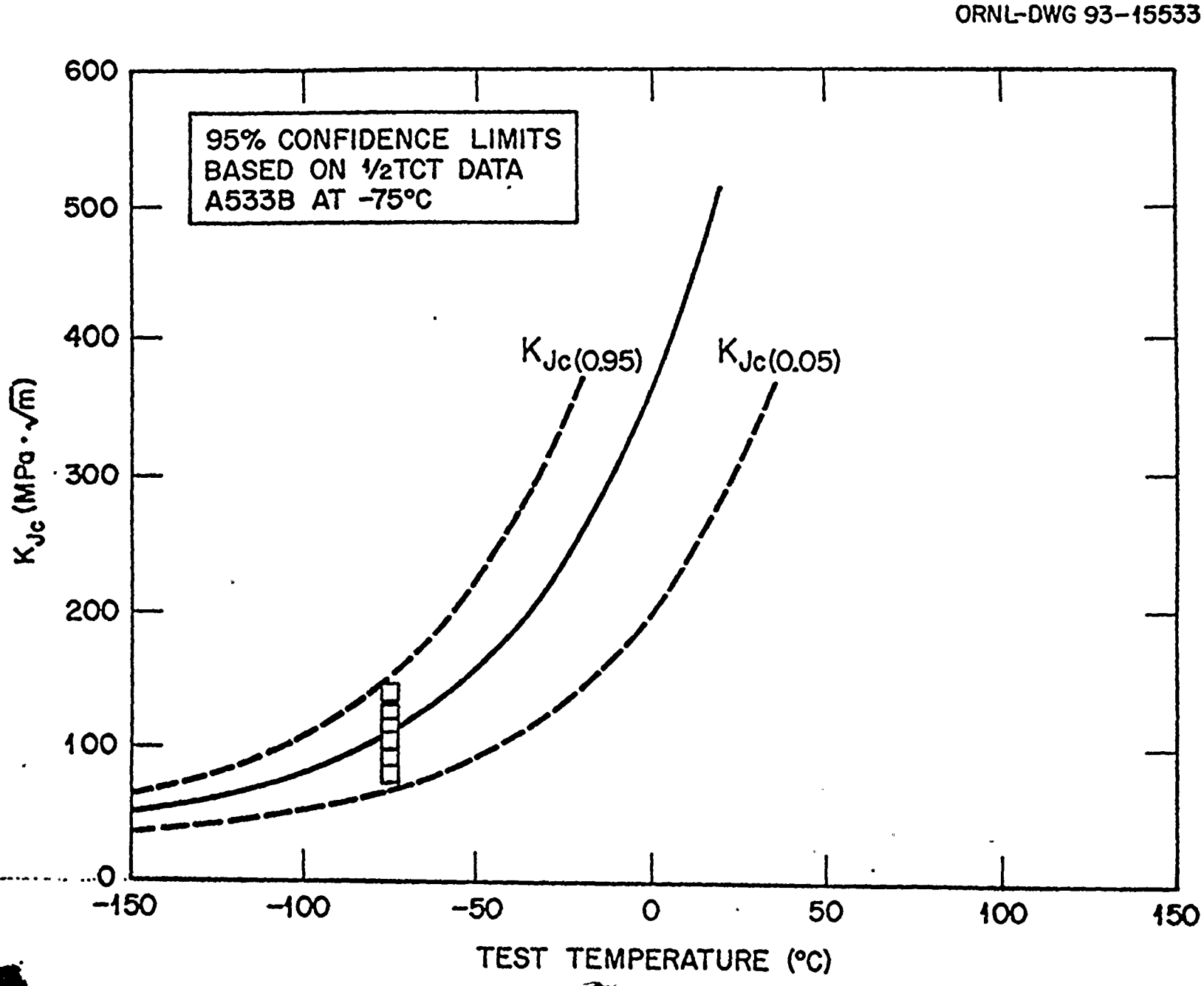

Fig. C1. Master curve with upper- and lower-bound 95% confidence limits.

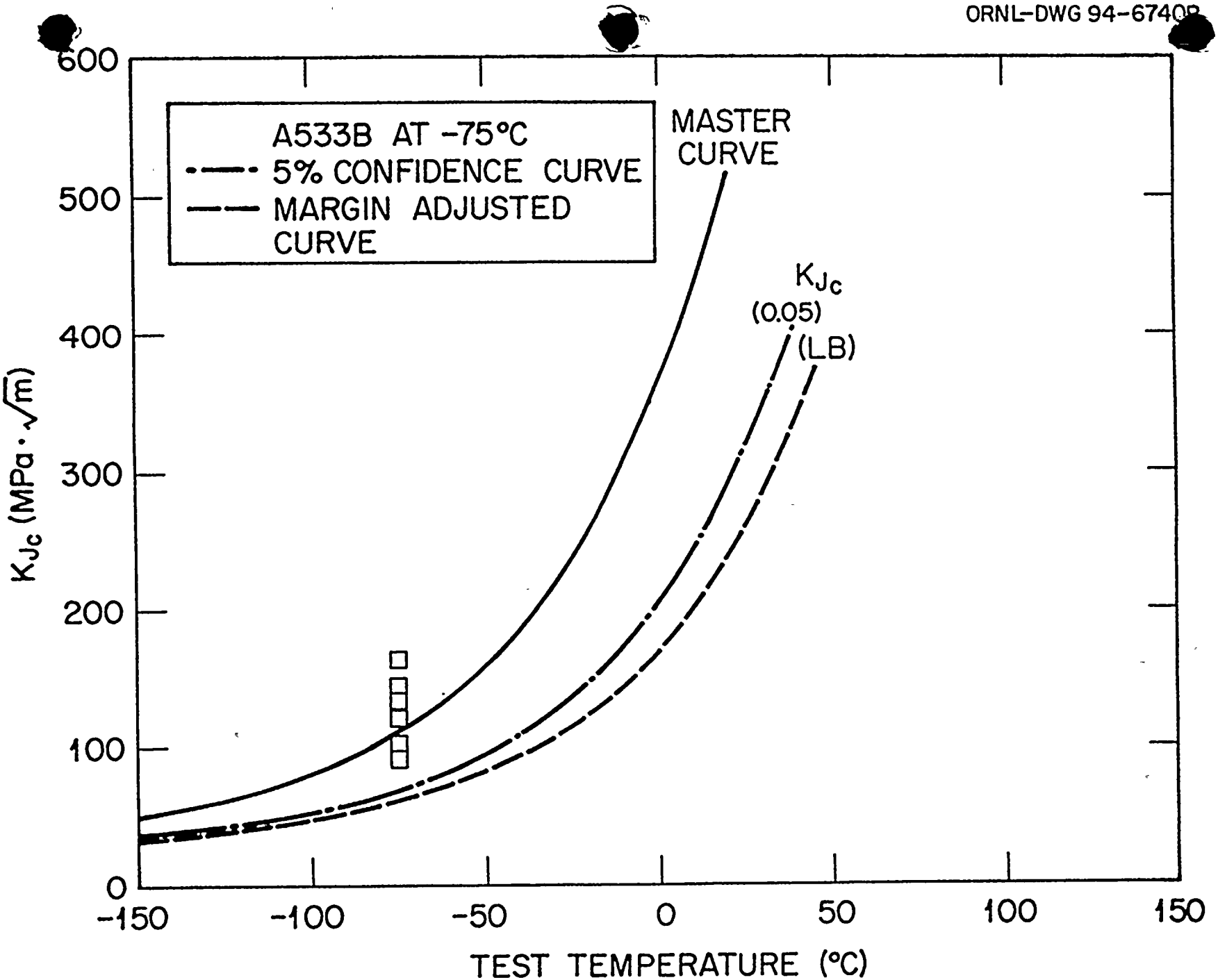

Fig. C2. Master curve showing the difference between 5% confidence limit and for lower bound that includes 85% confidence margin on T_o.